Summer 2015

Examination of the Cytotoxicity of Carboxyl Functionalized Single-Walled Carbon Nanotubes on Escherichia Coli

Brittany Linn Twibell

EXAMINATION OF THE CYTOTOXICITY OF CARBOXYL FUNCTIONALIZED SINGLE-WALLED CARBON NANOTUBES ON *ESCHERICHIA COLI*

A Masters Thesis

Presented to

The Graduate College of

Missouri State University

In Partial Fulfillment

Of the Requirements for the Degree

Master of Natural and Applied Sciences

By

Brittany Linn Twibell

July 2015

EXAMINATION OF THE CYTOTOXICITY OF CARBOXYL FUNCTIONALIZED SINGLE-WALLED CARBON NANOTUBES ON *ESCHERICHIA COLI*

Biology

Missouri State University, July 2015

Master of Natural and Applied Sciences

Brittany Linn Twibell

ABSTRACT

The growing use of carbon nanotubes (CNTs) in industrial and consumer products raises important questions about their environmental fate and impact on prokaryotes. In the environment, CNTs are exposed to a variety of conditions (e.g. UV light) that could lead to decomposition and changes in their chemical properties. Therefore, the potential cytotoxic effect of both pristine and artificially aged carboxyl functionalized single-walled CNTs at neutral and acidic conditions on *Escherichia coli* K12 was analyzed using a minimal inhibitory concentration (MIC) assay, which also allowed monitoring of non-lethal growth effects. However, there were no observable MIC or significant changes in growth behavior in *E. coli* K12 when exposed to pristine or aged CNTs. Exposure to pristine CNTs did not appear to influence cell morphology or damage the cells when examined by electron microscopy. In addition, RNA sequencing revealed no observable regulatory changes in typical stress response pathways. This is surprising considering that previous studies have claimed high cytotoxicity of CNTS, including carboxyl functionalized single-walled CNTs.

KEYWORDS: carbon nanotubes (CNTs), bacterial cytotoxicity, single-walled carbon nanotubes (SWCNTs), antibacterial, nanomaterials

This abstract is approved as to form and content

_____

Dr. Paul Schweiger
Chairperson, Advisory Committee
Missouri State University

EXAMINATION OF THE CYTOTOXICITY OF CARBOXYL FUNCTIONALIZED SINGLE-WALLED CARBON NANOTUBES ON *ESCHERICHIA COLI*

By

Brittany Linn Twibell

A Masters Thesis
Submitted to the Graduate College
Of Missouri State University
In Partial Fulfillment of the Requirements
For the Degree of Master of Natural and Applied Sciences

July 2015

Approved:

_____
Paul Schweiger, PhD

_____
Kyoungtae Kim, PhD

_____
Erich Steinle, PhD

_____
Julie Masterson, PhD: Dean, Graduate College

ACKNOWLEDGEMENTS

I would like to take this opportunity to express my gratitude to Dr. Schweiger for being an absolutely amazing mentor and providing his support and guidance throughout my graduate research. I would also like to express my appreciation to my committee members Dr. Kim and Dr. Steinle, as I have gained so much from their courses throughout my undergraduate and graduate studies at Missouri State University. I would like to thank Angela Schmoldt and Raymond Hovey at the University of Wisconsin-Milwaukee for their RNA sequencing work. I also want to acknowledge our lifecycle analysis collaborators at Missouri State University and Jordan Valley Innovation Center, with a special thank you to Rishi Patel for his electron microscopy work. In addition, I would like to thank the College of Natural and Applied Science for funding my research.

Finally, to the remarkable people that I call lab mates, thank you for making those long days and nights in lab all the more enjoyable.

TABLE OF CONTENTS

LIST OF TABLES

LIST OF FIGURES

1 INTRODUCTION

1.1 Overview of Carbon Nanotubes (CNTs)

Carbon nanotubes (CNTs) are a type of nanoparticle with the potential for many technological applications, but also have unknown toxicity. CNTs are cylinders of various lengths composed of single layers of carbon, called graphene, and can be single-walled (SWCNTs) or multi-walled CNTs (MWCNTs) with different chiralities based on the graphene structure used in the manufacturing process (Dai 2002; Petersen et al. 2011). Raw CNTs are synthesized by three main methods: laser vaporization, dc-arc discharge, and chemical vapor deposition and of these methods, dc-arc discharge and laser vaporization are the preferred methods for producing SWCNTs and tend to be used in large scale production (Dai 2002; Puretzky et al. 2000). During synthesis, carbon sources (either solid state or gaseous hydrocarbons, depending on the synthesis method) are used along with metal catalysts, such as cobalt, yttrium, iron and nickel catalysts, which can lead to raw CNTs having metal impurities (Kolosnjaj-Tabi et al. 2012; Puretzky et al. 2000; Köhler et al. 2008).

Raw CNTs are insoluble in aqueous solutions, causing precipitation and clumping of the material. However, solubility and dispersion can be improved when they are modified with functional groups, such as carboxyl groups (Kolosnjaj-Tabi et al. 2012; Chen et al. 2011). There are several routes for functionalization of CNTs, though common practices include acid treatment, such as sulfuric and nitric acid, along with heat treatment (Chen et al. 2011). The addition of functional groups to CNTs increase their potential applications by allowing them to bind macromolecules (Kolosnjaj-Tabi et al.

2012; Chen et al. 2011).

The industrial and commercial usage of CNTs has increased several fold over the past decade, and the research and development of new products incorporating CNT materials is swiftly growing. CNTs are used as additives in composite materials, such as CNT resins, that are used for a variety of products from wind turbine blades to sporting good equipment (De Volder et al. 2013). CNTs have also been used as additives in different types of coatings and films, such as protective paints containing MWCNTs, which are used in the marine industry and solar cells (De Volder et al. 2013; Köhler et al. 2008). Recent development of flexible touch screen displays that include SWCNTs have the potential to replace traditional indium tin oxide coated displays which are more brittle than the SWCNT counterparts (De Volder et al. 2013). Due to their high conductivity, stability, and higher energy density per mass unit compared to graphene, SWCNTs have been incorporated into the electrodes of lithium ion secondary batteries and greater than 60% of cell phone and tablet devices on the consumer market that use these types of batteries contain CNTs (Köhler et al. 2008). There is also interest in the use of CNTs in biosensor and drug delivery systems based on functionalization (De Volder et al. 2013). Despite the broad applications of CNTs, many questions remain about environmental and human safety, particularly for CNTs that can be directly released into the environment or come in direct contact with humans.

1.2 Current State of CNT Toxicity and Comparisons to Other Nanoparticles

Over the past several years many studies have been published in regards to CNTs and their potential effects and cytotoxicity, with a specific focus on human health

impacts. Significant decreases in cell viability and overall cytotoxic effects of SWCNTs in eukaryotic cell lines have been reported with exposure to concentrations at and above 100 μg/mL, and cytotoxic effects reported as reduced phagocytosis activities in alveolar macrophage cell lines after exposure to concentrations as low as 0.38 μg/mL (Lewinski et al. 2008; Jia et al. 2005). It has been reported that functionalization of SWCNTs can affect the observed cytotoxicity in human cell lines, with a higher degree of functionalization in a SWCNT product correlating with a lower observed percent cell death (Sayes et al. 2006). In addition, functionalized SWCNTs, including those with carboxyl groups, have been reported to have no significant cytotoxic effects in human cell lines in comparison to non-functionalized SWCNTs (Kam et al. 2004). Since CNTs are particles with similar physical characteristics to asbestos, the toxic effects of these two particles have been compared. Indeed some MWCNTs have been shown to cause comparable damage to human bronchial epithelia cells lines as asbestos (Kim et al. 2012).

Antibacterial properties of CNTs have been shown to be dependent on the various physicochemical characteristics of the CNTS, including length, diameter, and functional groups, as well as the type of bacteria being tested. SWCNTs have demonstrated antimicrobial affects by damaging bacterial cell membranes (Kang et al. 2007). Additionally, non-functionalized SWCNTs with diameters ranging from 1.04- 1.17 nm have been shown to cause damage to bacterial cell walls via piercing, which can lead to loss of cellular contents and cell death (Kang et al. 2007; Liu et al. 2009; Chen 2013). Coccoid bacteria with spherical morphology have been shown to be more susceptible to cellular damage and have lower survival rates in comparison to bacilli under the same

treatment conditions (Chen et al. 2013). It has been suggested gram positive bacteria are more susceptible to SWCNT damage (Liu et al. 2009), although the exact concentration of carboxyl-functionalized SWCNTs that inhibit bacterial growth in model bacterial organisms has yet to be adequately evaluated.

1.3 Environmental Life Cycle Assessment

Materials within the nanoscale range have high surface area as well as chemical and physical properties that differ from the same type of bulk material, which lends to the question of potential impacts for humans and ecosystems from nanomaterials like CNTs (US EPA 2010; Reinhart et al. 2010). Current standards and regulations on nanoparticles usually relate back to the bulk material properties since the United States Environmental Protection Agency (EPA) does not consider the particle size, only the molecular composition in their regulatory inventory list (US EPA 2008). CNTs are considered chemicals with a unique molecular identity under the Toxic Substances Control Act (TSCA), and as of 2013 the EPA has implemented a significant new use rule (SNUR) under the TSCA which specifically refers to CNTs (US EPA 2008; US EPA 2015). This SNUR allows the EPA to track and review chemicals before manufacturing or importing and make decisions based on potential impacts to human and ecosystems, and specifically cites concerns about chemicals generically identified as functionalized MWCNTs (US EPA 2015).

The EPA recognizes the need for further research on the impact of nanoparticles, including different classes of CNTs. One route that is of interest is a lifecycle analysis, which looks at impacts of a chemical and potential release points from production of the

raw materials, use in products, end of life recycling and disposal methods, and waste produced at any step in the life cycle (US EPA 2010; Köhler et al. 2008). As part of a lifecycle analysis it is important to consider how a chemical is incorporated into products, various environmental conditions that a chemical may experience, and also the impacts on organisms within potentially affected ecosystems. The effect of CNTs on the growth and viability on the environmental bacterial community is a key part of an environmental life cycle assessment of chemicals as bacteria are the most important biological factor in nutrient cycling.

When materials are deposited in the environment they are exposed to weathering processes that can be mimicked with the use of a UV accelerated weathering chamber (Grujicic et al. 2003). UV-light exposure has been shown to cause physical changes in CNT shape and chemical changes, including changes in the way oxygen associates with the carbon nanotube wall surfaces (Grujicic et al. 2003). The alterations in physical and chemical properties of aged CNTs lends to the question of whether environmental induced changes could affect cytotoxicity of CNTs. However, no studies on the effects of aged carboxyl functionalized SWCNTs on bacterial cytotoxicity have been done to date.

1.4 Determination of Cytotoxicity and Non-Lethal Effects of CNTs

The growth behavior, metabolism, and gene regulation of the model organism *Escherichia coli* K12 is well established, which makes it a common first choice microbe for cytotoxicology studies. It is predicted that exposure to pristine or aged carboxyl functionalized SWCNTs will have deleterious growth effects on *E. coli* K12 if they are cytotoxic. In this study, the ability of pristine and aged carboxyl functionalized SWCNTs

to inhibit *E. coli* K12 growth or cause cell death was monitored by a minimal inhibitory concentration (MIC) assays using a range of CNT concentrations using the CNTrene® C100LM SWCNT supplied by Brewer Science. The change in cell viability of *E. coli* K12 after exposure to concentrations of pristine carboxyl functionalized SWCNTs greater than 1.05 μg/mL was monitored by antibacterial plate testing. The effect of exposure to non-lethal concentrations of carboxyl-functionalized SWCNTs on cell morphology was evaluated by electron microscopy. Gene expression of *E. coli* K12 cells post CNT exposure was evaluated and compared to native gene expression by RNA sequencing. These results are expected to provide insights into the microbiological safety of this product that is potentially useful in commercial products such as advanced memory devices for computers, tablets, smart phones, and digital cameras.

2 MATERIALS AND METHODS

2.1 Bacteria and Media

Escherichia coli K12 strain SMG 123 (PTA7555) was grown in lysogeny broth (LB), which is a rich bacteriological medium, as well as M9 minimal salts medium with the addition of thiamine (M9+B1), which is a minimal medium that has no free proteins in solution. *E. coli* was grown at 37 °C and 200 rpm in a Thermo Scientific MaxQ 400 incubator shaker unless stated otherwise.

Lysogeny broth (LB)	
Tryptone	10 g
Yeast Extract	5 g
NaCl	10 g
H_2O_{dist}	Add to 1000 mL

For plates 15g agar was added to the medium prior to autoclaving

5X M9 Stock	
$Na_2HPO_4 \cdot 7H_2O$	64 g
KH_2PO	15 g
NaCl	2.5 g
NH_4Cl	5 g
H_2O_{dist}	Add to 1000 mL

1X M9 Solution	
5X M9 stock	200 mL
H_2O_{dist}	Add to 1000 mL

M9 Minimal Medium (M9+B1)	
1X M9 solution	1000 mL
1M $MgSO_4$ (filter sterilized)	2 mL
20% (w/v) glucose (filter sterilized)	20 mL
1M $CaCl_2$ (filter sterilized)	100 µL
1M Thiamine (filter sterilized)	1 mL

1X M9 solution was autoclaved prior to adding filter sterilized components

2.2 Carbon Nanotubes

CNTrene® C100LM carbon nanotubes (CNTs) were supplied by Brewer Scientific. CNTrene® C100LM is a pristine, carboxyl functionalized single-walled carbon nanotube (SWCNT) product suspended in water at a concentration of 135 µg/mL. CNTrene® C100LM has a length range of 0.4- 1.5 µm (90% of CNTs), a diameter range of 0.7- 3 nm (95% of CNTs), and a total metal ion content of less than 25 ppb (R. Patel, unpublished data). The pristine product is made up of SWCNT, DWCNT, and MWCNT at 70%, 25%, and 5% respectively (R. Patel, unpublished data). Pristine CNTs were aged in a QUV Accelerated Weathering chamber using a wavelength of 340 nm for 120 hours of direct exposure to simulate UV-A exposure. Aged CNTs were a generous gift from Dr. Adam Waynekaya (Missouri State University, Chemistry Department). Both pristine and aged CNTs were serially diluted in growth medium to final concentrations ranging from 33.75 µg/mL to 6.44 x 10^{-5} µg/mL for cytotoxicity assays.

2.3 Minimal Inhibitory Concentration (MIC)

A MIC assay was used to determine the minimum concentration of CNTs that completely inhibit the growth of *E. coli* K12 in liquid medium. To standardize the

inoculum used for MIC assays, preliminary standard plate counts were used to determine the colony forming units per milliliter (CFU/mL) of *E. coli* K12 in 100 mL of neutral (pH 7) growth medium (either LB or M9+B1) after an 18-20 hour incubation period at 37 ^{o}C at 200 rpm in a Brunswick Scientific G24 environmental incubator shaker. The calculated CFU/mL were also related back to the average OD_{600nm} (Shimadzu UV-1601 spectrophotometer) measured for the *E. coli* K12 cultures used for standard plate counts, which allowed for cultures to be verified before use for as standard inoculum in MIC assays. Once the average CFU/mL was determined for both types of growth media, the final cell number added to each assay was adjusted to a standard inoculum of 5.00×10^5 CFU/mL, which was calculated based on the following formula:

$$C_1V_1 = C_2V_2$$

In the above equation, C_1 is initial concentration of bacterial cells, V_1 is the volume of C_1 being used for the dilution, C_2 is the target concentration of bacterial cells, and V_2 is the final volume of the culture including V_1.

A broth micro dilution MIC assay on a 96-well transparent C-bottom plate was performed with a standard inoculum of 5.00×10^5 CFU/mL (based on preliminary standard plate counts) in a final reaction volume of 200 µL (Wiegand et al. 2008). Medium used included LB under neutral and acidic conditions (pH 7 and pH 5 respectively) as well as M9+B1 at neutral conditions (pH 7). A BioTek EL808 plate reader was used to monitor optical density at 595 nm (OD_{595}). Plates were incubated at 37 ^{o}C at the medium shake rate of the instrument for 24 hours with OD_{595} readings taken every 30 minutes. The Gen5 software was used for data collection.

Each plate had a negative control in column 12, with only growth medium to

validate sterility during plate setup and inoculation (Figure 1). In column 11 a positive control with growth medium inoculated with *E. coli* K12 was used as a normal growth comparator. Row A and row E were CNTs blanks, comprised of growth medium and CNT dilutions, which allowed correction of the intrinsic CNT background absorbance. Experimental wells were inoculated with *E. coli* K12 and contained CNT dilutions from 33.77 μg/ml to 6.44 x 10^{-5} μg/ml and were assayed in triplicate. Each CNT dilution was also assayed with three biological replicates (n=9).

Growth curves were generated by monitoring OD_{595nm}. Doubling times (t_d) were calculated based on the following formulas:

(1) $N = N_o 2^n$; where N is the final OD at time t, N_o is the initial OD, and n is the number of generations per unit time.

(2) Rearrangement of (1) gives: $n = \log (N/N_o) / 0.301$

(3) $t_d = t/n$ or $n = t/t_d$; where t_d is doubling time

(4) substituting (2) for (3) gives: $t_d = 0.301t / (\log N - \log N_o)$

Growth curves and doubling times were used to evaluate nonlethal growth effects of CNT exposure.

2.4 Antibacterial Plate Counts

The effect of pristine CNT concentrations greater than 5 μg/mL on the growth of *E. coli* K12 was evaluated by the spot-plate technique using a modified method of Gaudy et. al., 1963. *E. coli* K12 cultures were inoculated in 96-well transparent C-bottom plates with LB (pH 7) and pristine CNTs (0 μg/mL, 8.44 μg/mL, 16.88 μg/mL, and 33.75 μg/mL) in triplicate to a final volume of 200 μL and incubated for 24 hours at 30 ^oC and

200 RPM in a Lab-Line 3525 orbit incubator shaker. Serial ten-fold dilutions of overnight cultures were performed on 96-well plates and 10 µl of the 10^{-5}, 10^{-6}, and 10^{-7} dilutions were spotted in triplicate on LB plates and incubated at 30 ºC for 16-18 hours. Colony forming units per milliliter (CFUs/mL) were calculated for each concentration of CNTs and compared to that of the unexposed control group.

2.5 Electron Microscopy

Morphological change of bacterial cells exposed to CNTs was evaluated by scanning electron microscopy (SEM) and atomic force microscopy (AFM). A serial ten-fold dilution of an overnight 5 mL LB (pH 7) culture of *E. coli* K12 was performed, and 100 µL from the 10^{-3} dilution was used to inoculate LB (pH 7) in a final volume of 200 µl in a 96-well transparent C-bottom plate. Medium also contained 0 µg/mL, 33.75 µg/mL, 16.88 µg/mL, and 1.05 µg/mL pristine CNTs. *E. coli* K12 was grown at each CNT concentration in triplicate for 24 hours. All electron microscopy sample preparation steps were done at room temperature. Replicates were combined, pelleted by centrifugation at 5000 x g for 5 minutes, and then washed three times in 0.1 M phosphate buffer (pH 7.2) to remove growth medium. Cells were dehydrated by an ascending ethanol wash series (50%, 70%, 80%, 90%, 95%, 100%, and 100%) with a 5 minute exposure to each concentration of ethanol. Samples were transferred onto silicon wafers in 10 µL volumes and either frozen in liquid nitrogen and freeze dried overnight for SEM or allowed to air dry overnight for AFM.

Prepared samples were visualized on instruments located at the Jordan Valley Innovation Center by Rishi Patel. Samples were visualized with the JEOL JSM-7600F

field emission scanning electron microscope under vacuum (9.6 x 10^{-5} Pascal). SEM images were captured using an accelerating voltage of 1.00 kV and a working distance (WD) between 5.1 mm and 5.2 mm at total magnification ranging from 10,000x to 20,000x. AFM imagines were captured utilizing the Veeco Dimension 3100 with a Nanoscope IIIA Controller under atmospheric conditions (1.01 x 10^5 Pascal). AFM imagines were captured on tapping mode (scan size 5.000 μm or 20.0 μm, scan rate 1.001 Hz, 512 samples) using a silicon tip with a nominal radius of 8.0 nm.

2.6 RNA Sequencing

Gene expression of CNT exposed bacterial cells was evaluated with RNA sequencing and compared to native gene expression. The RNeasy Plus Mini Kit (Qiagen, Venlo, Netherlands) recommends the use of minimal medium for culturing bacteria. Fifty microliters from overnight cultures of *E. coli* K12 in 5 mL of M9+B1 was inoculated into 5 mL of M9+B1 medium in disposable 16 mL culture tubes. Pristine CNTrene® C100LM was added to 1.05 μg/mL to experimental cultures. Bacterial cultures were incubated for 6 hours to mid-log phase with each sample grown in duplicate. The RNeasy Plus Mini Kit (Qiagen) was used to extract RNA from 2 mL of culture with one on-column treatment with the RNase-Free DNase Set (Qiagen) according to the manufacturer's instructions. RNA extractions were carried out in duplicate for each culture.

RNA concentrations were evaluated using the IMPLEN nanophotometer (RNA function, lid factor 10, 2 μL sample). To confirm samples were of high quality, the RNA was also analyzed with an Agilent Technologies 2100 Bioanalyzer system and 2100

Expert software (Dr. Wenping Qiu, Missouri State University, Agriculture Department). Samples were concentrated by evaporation at room temperature overnight in a class 2 A laminar flow hood to provide sufficient volume and concentration required for ribosomal depletion.

Ribosomal depletion was done using the bacterial Ribo-Zero rRNA Removal Kit (Illumina, San Diego, Ca, USA) according to the manufacturer's instructions. The SMARTer Stranded RNA-Seq kit (Clontech, Mountain View, Ca, USA) was used to prepare cDNA from high quality RNA samples according to the manufacturer's instructions. An Illumina MiSeq instrument (single-end 50 base pair read length) was used for RNA sequencing. Sequencing data was analyzed using the DNAstar Lasergene Suite Qseq software (http://www.dnastar.com). The sequence reads were mapped and analyzed using the RNA-Seq pipeline default parameters using *E. coli* K12 MG1655 as a reference genome.

2.7 Waste Handling

All waste that came in contact with CNTrene® C100LM materials, including bacterial cultures, were collected by Environmental Management and processed as hazardous material. Liquid waste was stored in a labeled glass container in a ventilation hood until collected for processing. Solid waste was double bagged (e.g. 96 well plates, gloves, and microcentrifuge tubes) and sealed in in a bag-lined 5 gallon bucket with a screw-top lid until waste collection by Missouri State University Environmental Management.

2.8 Data Analysis

Comparison of doubling times calculated from growth curves were evaluated by Pearson's correlation coefficient using Social Science Statistics using $p = 0.01$ as threshold for statistical significance (Jeremy Stangroom ©2015, URL http://www.socscistatistics.com), as well as regression analysis using GraphPad Prism 5 software (GraphPad Software Inc. ©2015, La Jolla, CA). Evaluation of differences in CFU/mL from antibacterial plate testing was done by unpaired t-test (two-tailed p-value with 95% confidence levels) using Quick Calc GraphPad software (GraphPad Software Inc. ©2015). All graphs were generated using Microsoft Excel, with the exception of the box-whisker plot, which was generated using the R programming language (R Core Team, 2013). RNA sequencing data was analyzed using the student t-test with the false discovery rate restricted to 0.05 using the Benjamini Hochberg method as the P-value adjustment method (Benjamini and Hochberg 1995).

		1	2	3	4	5	6	7	8	9	10	11	12
CNT Blank row (µg/mL)	**A**	33.75	16.88	8.44	4.22	2.11	1.05	0.53	0.26	0.13	6.59E-02	**Positive growth control**	**Negative growth control**
Experimental CNT (µg/mL)	**B**	33.75	16.88	8.44	4.22	2.11	1.05	0.53	0.26	0.13	6.59E-02		
Experimental CNT (µg/mL)	**C**	33.75	16.88	8.44	4.22	2.11	1.05	0.53	0.26	0.13	6.59E-02		
Experimental CNT (µg/mL)	**D**	33.75	16.88	8.44	4.22	2.11	1.05	0.53	0.26	0.13	6.59E-02		
CNT Blank row (µg/mL)	**E**	3.30E-02	1.65E-02	8.24E-03	4.12E-03	2.06E-03	1.03E-03	5.15E-04	2.57E-04	1.29E-04	6.44E-05		
Experimental CNT (µg/mL)	**F**	3.30E-02	1.65E-02	8.24E-03	4.12E-03	2.06E-03	1.03E-03	5.15E-04	2.57E-04	1.29E-04	6.44E-05		
Experimental CNT (µg/mL)	**G**	3.30E-02	1.65E-02	8.24E-03	4.12E-03	2.06E-03	1.03E-03	5.15E-04	2.57E-04	1.29E-04	6.44E-05		
Experimental CNT (µg/mL)	**H**	3.30E-02	1.65E-02	8.24E-03	4.12E-03	2.06E-03	1.03E-03	5.15E-04	2.57E-04	1.29E-04	6.44E-05		

Figure 1. Schematic of 96 well plate layout for MIC assay with CNTrene® C100LM

3 RESULTS

3.1 MIC Assays of *E. coli* K12 under Various Growth Conditions

Based on OD_{595nm} readings, a MIC value can be determined for each type of CNT for *E. coli* K12 under various growth conditions. A MIC value is the lowest concentration of the CNT treatment that completely inhibits bacterial growth, which would be seen as no change in optical density readings during the duration of the incubation period.

To standardize the inoculum used for the MIC microplate assays, the cell number had to be correlated to the colony forming units produced per milliliter of culture (CFU/mL). This was done by using a standard plate count for *E. coli* K12 grown in LB or M9+B1 at a neutral pH. After 18-20 hours of growth, the CFU/mL were correlated to the average OD_{600nm} of each media type. *E. coli* K12 cultures grown in LB (pH 7) medium had an average of 5.02×10^9 ($\pm 1.34 \times 10^9$) CFU/mL at an average OD_{600nm} of 2.32 ($\pm$ 0.03). A lower optical density (0.95 ± 0.07) and cell number ($6.13 \times 10^8 \pm 2.61 \times 10^8$) was observed when *E. coli* K12 was grown in M9+B1 medium, pH 7. Once the average CFU/mL was determined for both types of growth media, the final cell number added to each MIC assay was adjusted to a standard inoculum of 5.00×10^5 CFU/mL.

Growth curves for *E. coli* K12 were generated by plotting the natural logarithm of the OD_{595nm} over a 24 hour period. Microtiter wells containing only growth medium and either pristine or aged CNTrene® C100LM at each treatment concentrations were subtracted from their respective data sets to normalize bacterial growth for intrinsic absorbance of the media and/or the CNTs. Doubling times were calculated as previously described (see section 2.3) for *E. coli* K12 under various growth conditions. Due to

significant optical interference from CNTrene® C100LM at concentrations higher than 1.05 μg/mL, only exposure to concentrations ranging from 6.44 x 10^{-5} μg/mL to 1.05 μg/mL were considered in doubling time calculations.

Growth curves for *E. coli* K12 in LB (pH 7) in the presence of pristine CNTs over the tested concentration range were very similar to the growth observed in the control groups, with all growth curves overlapping (Figure 2-3). The same trend was observed for *E. coli* K12 in LB (pH 7) in the presence of aged CNTs, with growth curves for controls and treatment groups overlaying (Figure 4-5). Cultures in LB (pH 7) had doubling times ranging from 21.4 min to 26.1 min (± ≤ 1.7 min) after exposure to pristine CNTs, and doubling times ranging from 20.9 min to 24.1 min (± ≤ 1.6 min) when exposed to aged CNTs (Figure 6). In comparison, control groups in the pristine and aged CNT assays had doubling times of 23.2 min (± 0.7 min) and 22.2 min (±0.5 min) respectively with an overall average of 22.7 min (± 0.8 min) (Figure 6). Even the highest doubling time observed at 26.1 min (± 1.2 min) (1.05 μg/mL pristine CNT) was still within 3.4 min of the overall doubling time for the control groups.

Doubling times observed for *E. coli* K12 in LB (pH 7) were similar between pristine and aged CNTs at the same treatment concentrations, with percent differences ranging from 0.8% to 5.8%, with the exception of the 1.05 μg/mL and 5.15 x 10^{-4} μg/mL concentrations (13.6% and 9.7% respectively) (Table 1). The percent difference between controls from the pristine CNT assays and the aged CNT assays was 4.5%, indicating that the differences observed between pristine and aged CNTs was within typical experimental deviation (Table 1). There was a moderate positive correlation between pristine CNT concentration and doubling time in *E. coli* K12 growth in LB (pH 7) (p =

0.000148, $R^2 = 0.276$). However, only 27.6% of the variation was explained by the CNT concentrations tested, and no correlation was observed when the highest pristine CNT concentration (1.05 μg/mL) was omitted from the analysis ($p = 0.357281$, Pearson correlation coefficient) (Figure 7). These data suggest that the observed increase in doubling time may be due to minor intrinsic optical interference in optical density measurements, likely due to the CNTs being black and having a tendency to flocculate. In contrast, there was no significant correlation between the concentration of aged CNTs and doubling time under the same conditions ($p = 0.081$, Pearson correlation coefficient) (Figure 7).

Growth curves for *E. coli* K12 in M9+B1 minimal medium in the presence of either pristine or aged CNTs over the tested concentration range were very similar to the growth observed in the control groups, with all growth curves in both data sets overlapping (Figure 8-11). Since M9+B1 is a minimal medium, observed doubling times were higher than those observed in the nutrient rich LB medium. Control groups in the pristine and aged CNT assays had doubling times of 60.9 min (± 0.6 min) and 60.3 min (± 1.0 min) respectively with an overall average of 60.7 min (± 0.7 min) among control groups (Figure 12). *E. coli* K12 cultures in M9+B1 that were exposed to CNTs had similar doubling times. Doubling times ranged from 59.2 min to 61.8 min (≤± 4.9 min) in the presence of pristine CNTs, and 58.7 min to 60.6 min (≤± 2.0 min) when exposed to aged CNTs (Figure 12).

The doubling times observed for *E. coli* K12 in M9+B1 were very similar between pristine and aged CNTs at the same treatment concentrations, with percent difference ranging from 0.3% to 4.0%, which was comparable to the percent difference of

1.0% observed between the controls from the pristine CNT and the aged CNT assays (Table 1).There was no significant correlation between the concentration of pristine CNTs and doubling time of *E. coli* K12 in M9+B1 medium ($p = 0.941385$, Pearson correlation coefficient) (Figure 13). Similarly, there was no significant correlation between the concentration of aged CNTs and doubling time ($p = 0.138074$, Pearson correlation coefficient).

Growth curves for *E. coli* K12 in LB (pH 5) in the presence of either pristine or aged CNTs over the tested concentration range were very similar to the growth observed in the control groups, with all growth curves in both data sets superimposing (Figure 14-15). Control groups in the pristine and aged CNT assays had doubling times of 30.1 min (± 1.0 min) and 29.1 min (± 0.1 min) respectively with an overall average of 29.5 min (± 0.7 min) among control groups (Figure 16). *E. coli* K12 cultures in LB (pH 5) that were exposed to either pristine or aged CNTs had doubling times ranging from 30.1 min to 31.7 min (≤± 1.5 min) and from 28.9 min to 31.5 min (≤± 1.3 min) respectively (Figure 16).

The doubling times observed for *E. coli* K12 in LB (pH 5) were very similar between pristine and aged CNTs at the same treatment concentrations, with percent difference ranging from 0.7% to 5.9% (Table 1). The percent difference between the controls from the pristine CNT and the aged CNT assays was 3.3% (Table 1). There was no significant correlation between the concentration of pristine CNTs and doubling time of *E. coli* K12 in LB (pH 5) medium ($p = 0.024581$, Pearson correlation coefficient) (Figure 17). In contrast, there was a significant correlation between the concentration of aged CNTs and doubling time under the same conditions ($p = 0.000031$, Pearson

correlation coefficient) (Figure 17). This is surprising since the percent difference between doubling times observed after pristine or aged CNT exposure was at most 5.9%, which was less than a two-fold increase of the percent difference observed between controls (3.3%). Furthermore, doubling times were only slightly increased (2.4 min longer) than the unexposed control, indicating that differences observed may be due to random experimental variation of the assay used.

3.2 Antibacterial Plate Counts

Significant optical interference was observed at CNT concentrations over 1.05 µg/mL, making MIC microtiter assays infeasible. Therefore, growth effects of pristine CNTs at concentrations higher than 1.05 µg/mL on *E. coli* K12 were evaluated by a modified spot plate technique (see section 2.6). The CFU/mL were calculated after 24 hours of exposure to pristine CNTs at final concentrations of 0 µg/mL (control), 8.44 µg/mL, 16.88 µg/mL, and 33.75 µg/mL. The calculated CFU/mL were 2.04×10^9 CFU/mL ($\pm 4.63 \times 10^8$ CFU/mL, n = 8), 1.26×10^9 CFU/mL ($\pm 3.72 \times 10^8$ CFU/mL, n = 11), 1.39×10^9 CFU/mL ($\pm 2.85 \times 10^8$ CFU/mL, n = 8), and 1.37×10^9 CFU/mL ($\pm 3.44 \times 10^8$ CFU/mL, n = 11), respectively (Figure 18). The colony forming units for *E. coli* K12 exposed to each treatment concentration of CNTs (8.44 µg/mL, 16.88 µg/mL, and 33.75 µg/mL) were found to be significantly different from the control group ($p = 0.0008$, $p = 0.0045$ and $p = 0.0021$; unpaired two-tailed t-test), respectively. Although these p-values suggest that there is a significant difference between the control and treatment groups, the difference was less than or equal to a 1.61-fold reduction in CFU/mL among the three treatment conditions. Furthermore, a linear regression of these data does not

significantly deviate from zero ($p = 0.4031$). Taken together, these data imply that there is no true biological significance in the slight reduction in CFU/mL when *E. coli* is exposed to up to 33.75 μg/mL CNTs.

3.3 Electron Microscopy Imagining

Morphological changes of *E. coli* K12 exposed to pristine CNTs at concentrations at and above 1.05 μg/mL were evaluated by electron microscopy. With SEM, control cells visualized at 10,000x and 25,000x appeared as morphologically normal bacilli, with intact outer membranes and lengths ranging between 1 μm and 2 μm (Figure 19). After 24 hour exposure to pristine CNTs (33.75 μg/mL and 16.88 μg/mL), cells had similar morphologies to control samples. The *E. coli* were within the typical 1 μm to 2 μm length range and had normal intact outer membranes, and physical damage caused by CNT exposure was not observed (Figure 19).

Three dimensional AFM images were generated by the Veeco Dimension 3100 with a Nanoscope IIIA Controller using tapping mode (scan size 5.000 μm or 20.0 μm; scan rate 1.001 Hz, 512 samples) and a silicon tip (radius of 8.0 nm) under atmospheric conditions. As was observed with SEM, AFM images of control *E. coli* K12 cells appeared as morphologically normal bacilli with intact outer membranes, lengths between 1 μm to 2 μm, and diameters of 0.5 μm (Figure 20-21). After 24 hour exposure to pristine CNTs (33.75 μg/mL, 16.88 μg/mL, and 1.05 μg/mL), cells had normal morphological features including cell length and diameter (1 μm – 2 μm and 0.5 μm, respectively), similar to control cells (Figure 20-21).

In SEM images, CNTs were primarily observed to be adjacent to bacterial cells

and not in direct contact with the cell surface. Although, some CNTs were in direct contact with outer membranes of the cells, yet no damage to outer membranes, such as physical puncturing, was observed. Due to the resolution restrictions of the instrument, no CNT structures could be positively identified in AFM images, so no association between cells and CNTs was directly observed. However, cells appeared intact, without abnormalities in cell morphology, which corresponds to the SEM images. Taken together, these data suggest that the CNTs are do not physically damaging *E. coli*.

3.4 RNA Sequencing

RNA sequencing was carried out for *E. coli* K12 cultures grown to mid-log phase in M9+B1 minimal medium, with experimental cultures exposed to pristine CNTs at a concentration of 1.05 µg/mL and compared to control cultures without CNT exposure. RNA extracts were analyzed with an IMPLEN nanophotometer and an Agilent Technologies 2100 Bioanalyzer system. Total RNA concentrations of samples ranged from 14 ng/µL to 22 ng/µL when evaluated with the nanophotometer. RNA concentrations largely agreed when analyzed with the Bioanalyzer, and were all determined to be between 10 ng/µL to 16 ng/µL using this system (Table 2). Electropherograms from the Bioanalyzer showed strong peaks corresponding to 16S rRNA and 23S rRNA regions and were centered around 40 seconds and 45 seconds, respectively (Figure 22). The 16S and 23S rRNA migrated to the expected size according to the simulated Bioanalyzer gel images. The ratio of the 16S and 23S rRNA areas were used by the 2100 Expert Software to determine the RNA integrity number (RIN) of the sample. An RIN with a value greater than or equal to 8 was considered high quality and

suitable for library construction (Agilent, 2005). All RNA extracts had rRNA ratios (16S/23S) ranging from 1.4 to 1.8 with RIN values ranging from 8.9 to 9.3 (Table 2). Taken together, these data indicated that the total RNA preparations were not degraded and of high quality, suitable for RNA-seq library preparation.

After ribosomal depletion, RNA samples were again evaluated with an Agilent Technologies 2100 Bioanalyzer system to confirm rRNA was significantly reduced to increase reads aligning to coding mRNA, as around 80% of total RNA may be rRNA in *E. coli* (Giannoukos et al. 2012). Depleted RNA concentrations ranged from 170 pg/µL to 753 pg/µL, with rRNA contamination percentages ranging from 0.4% to 15.3% (Table 2). These data confirmed that rRNA was significantly depleted prior to library preparation and sequencing.

Control samples one through three had total aligned sequence reads of 1,898,979 reads, 2,154,777 reads, and 2,546,169 reads, respectively. Similarly, experimental samples one through three exposed to 1.05 µg/mL of pristine CNTs had total aligned sequence reads of 2,492,925 reads, 2,434,573 reads, and 2,849,043 reads, respectively. All control and experimental samples had sequence lengths of 35-51 bp with a GC content of approximately 54%, closely mirroring the genomic GC percentage of 50.8% (Riley et al. 2005). Gene expression of *E. coli* K12 exposed to pristine CNTs was compared to native gene expression with the *E. coli* K12 MG1655 reference genome used for mapping sequencing reads. Of the 4464 open reading frames (ORFs) (NCBI accession NC_000913), 4314 genes were mapped indicating that 96.6% of all genes were expressed. Of the 4314 genes mapped, 186 genes were differentially expressed using a 2-fold change between control and experimental samples as a threshold. Of these 186

genes, 26 genes were upregulated in the experimental CNT exposed samples, and 160 genes were downregulated (Figure 23). However, only three genes (*pptA, alpA,* and *mgtL*) were expressed at a significantly different level in the experimental samples after correcting for false discovery rate of 0.05 using the Benjamini-Hochberg method (Benjamini and Hochberg 1995). The *pptA* and *alpA* genes were considered significantly downregulated with a 2.5-fold change ($p = 0.0272$) and 35.1-fold change ($p = 0.0227$), respectively. The *mgtL* gene was the only gene to be upregulated, with an 85.3-fold increase in expression in experimental samples ($p = 1.87 \times 10^{-7}$) (Table 3).

The *pptA* gene (COG 1942) is predicted to encode a 4-oxalocrotonate tautomerase that functions in degradation pathways for xenobiotic aromatic compounds (Kanehisa and Goto 2000). The *alpA* gene (COG 3311) is prophage regulatory protein that is part of a group of DNA transcription regulators within the MerR superfamily, and regulators within this family have been shown to regulate in response to environmental stressors, such as heavy metals (Marchler-Bauer et al. 2015). The genes downstream of this ORF encode proteins associated with the cryptic prophage CP4-57. The *mgtL* gene acts as a leader sequence to the downstream *mgtA* gene (COG 0474) which is a Mg^{2+} transport protein (Park et al. 2010). The *mgtL* leader sequence serves a riboswitch for the Mg^{2+} porin, which allows expression of the porin to be regulated by the availability of proline and Mg^{2+} (Park et al. 2010).

Of these 3 genes, the *pptA* gene regulation was very close to the 2-fold change threshold and may not actually be differentially expressed. Therefore this genes should be verified by quantitative polymerase chain reaction (qPCR) to validate if is truly downregulated or the differential expression is due to experimental variation. Only the

alpA and *mgtL* genes showed high levels of differential expression after CNT exposure. Regardless, the role of all three genes identified by RNA-seq in response to CNT exposure is unclear as all three genes have dissimilar function and are not part of a general stress response that would be expected from physical interaction or cell envelope damage.

Table 1. Percent differences between doubling times for *E. coli* K12 exposed to either pristine or aged CNTrene® C100LM for 24 hours

	% Difference*		
CNT(μg/mL)	LB (pH 7)	LB (pH 5)	M9+B1
0 (Control)	4.5%	3.3%	1.0%
6.44×10^{-5}	1.5%	4.4%	0.4%
1.29×10^{-4}	5.8%	ND	0.6%
2.57×10^{-4}	1.4%	2.0%	0.8%
5.15×10^{-4}	9.7%	ND	1.2%
1.03×10^{-3}	1.8%	5.9%	1.7%
2.06×10^{-3}	0.8%	ND	1.3%
4.12×10^{-3}	2.8%	2.9%	1.1%
8.24×10^{-3}	3.6%	ND	1.0%
1.65×10^{-2}	3.9%	3.9%	0.3%
3.30×10^{-2}	2.9%	ND	1.0%
6.59×10^{-2}	2.2%	5.0%	3.4%
0.13	4.0%	2.5%	2.2%
0.26	1.8%	2.7%	3.0%
0.53	0.9%	0.7%	4.0%
1.05	13.6%	0.9%	0.4%

* Percent difference for CNT treatment samples was calculated by comparison between pristine and aged treatment groups; Percent difference for controls was calculated by comparison of independent control samples between the pristine and aged assay plates. ND, not determined for the concentration of CNTrene® C100LM in the specified growth medium

Table 2. RNA extracted from *E. coli* K12 quality control analysis

			Total RNA (ng/µL)			
Sample	RIN	rRNA ratio [23s/16s]	Nano-photometer	Bioanalyzer	rRNA Depleted RNA (pg/µL)	rRNA contamination
Control 1	9	1.4	14	13	170	0.4%
Control 2	8.9	1.6	22	15	211	3.4%
Control 3	9.2	1.6	15	14	499	2.5%
CNT 1	8.9	1.6	16	16	753	15.3%
CNT 2	9.2	1.6	14	11	407	8.3%
CNT 3	9.3	1.8	16	10	740	10.7%

RIN, RNA integrity number from Agilent 2100 Bioanalyzer

Table 3. Comparative gene expression in *E. coli* K12 based on RNA sequencing

Gene name	COG	Fold Change (experimental/ control)	Standard deviation		P-value
			Control	Experimental	
mgtL	0474*	85.3 up	0.0	0.053	1.87×10^{-7}
alpA	3311	35.1 down	0.816	0.0	0.0227
pptA	1942	2.5 down	0.172	0.138	0.0272

COG, Clusters of orthologous groups of proteins
* COG number for *mgtA* gene provided as *mgtL* is as a leader sequence for *mgtA* and does not belong to a COG family.

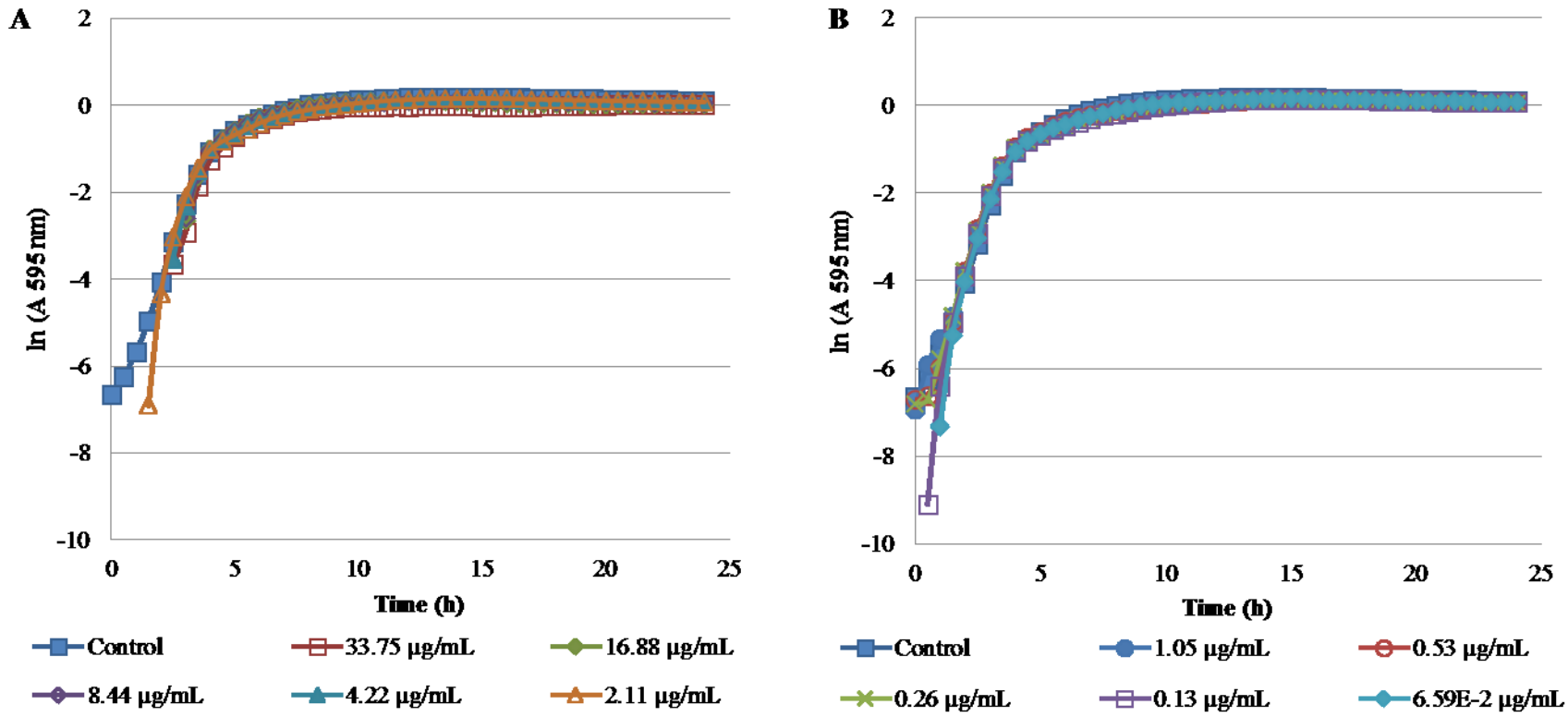

Figure 2. Growth curves of *E. coli* K12 in LB at pH 7 over a 24 hour period with pristine CNTrene® C100LM treatment at and above 6.59 x 10^{-2} µg/mL. Control cells were grown in medium without CNT treatment. Wells containing growth medium and pristine CNTrene® C100LM at treatment concentrations were subtracted from OD data sets in order to normalize background absorbance and distinguish bacterial growth. (A) Treated with 33.75 µg/mL, 16.88 µg/mL, 8.44 µg/mL, 4.22 µg/mL, and 2.11 µg/mL pristine CNTrene® C100LM; (B) Treated with 1.05 µg/mL, 0.53 µg/mL, 0.26 µg/mL, 0.13 µg/mL, 6.59 x 10^{-2} µg/mL pristine CNTrene® C100LM.

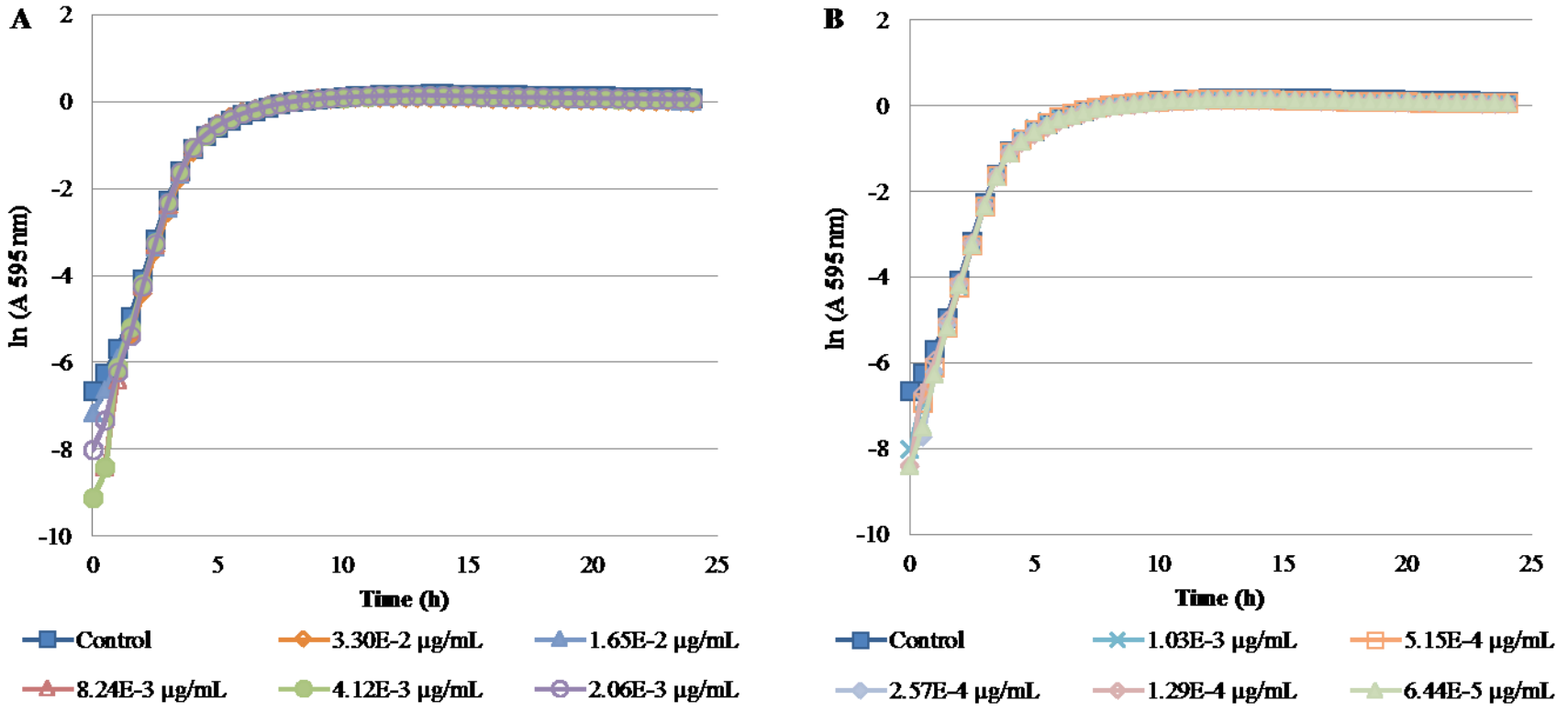

Figure 3. Growth curves of *E. coli* K12 in LB at pH 7 over a 24 hour period with pristine CNTrene® C100LM treatment at and below 3.30 x 10^{-2} µg/mL. Control cells were grown in medium without CNT treatment. Wells containing growth medium and pristine CNTrene® C100LM at treatment concentrations were subtracted from OD data sets in order to normalize background absorbance and distinguish bacterial growth. (A) Treated with 3.30 x 10^{-2} µg/mL, 1.65 x 10^{-2} µg/mL, 8.24 x 10^{-3} µg/mL, 4.12 x 10^{-3} µg/mL, and 2.06 x 10^{-3} µg/mL pristine CNTrene® C100LM; (B) Treated with 1.03 x 10^{-3} µg/mL, 5.15 x 10^{-4} µg/mL, 2.57 x 10^{-4} µg/mL, 1.29 x 10^{-4} µg/mL, and 6.44 x 10^{-5} µg/mL pristine CNTrene® C100LM.

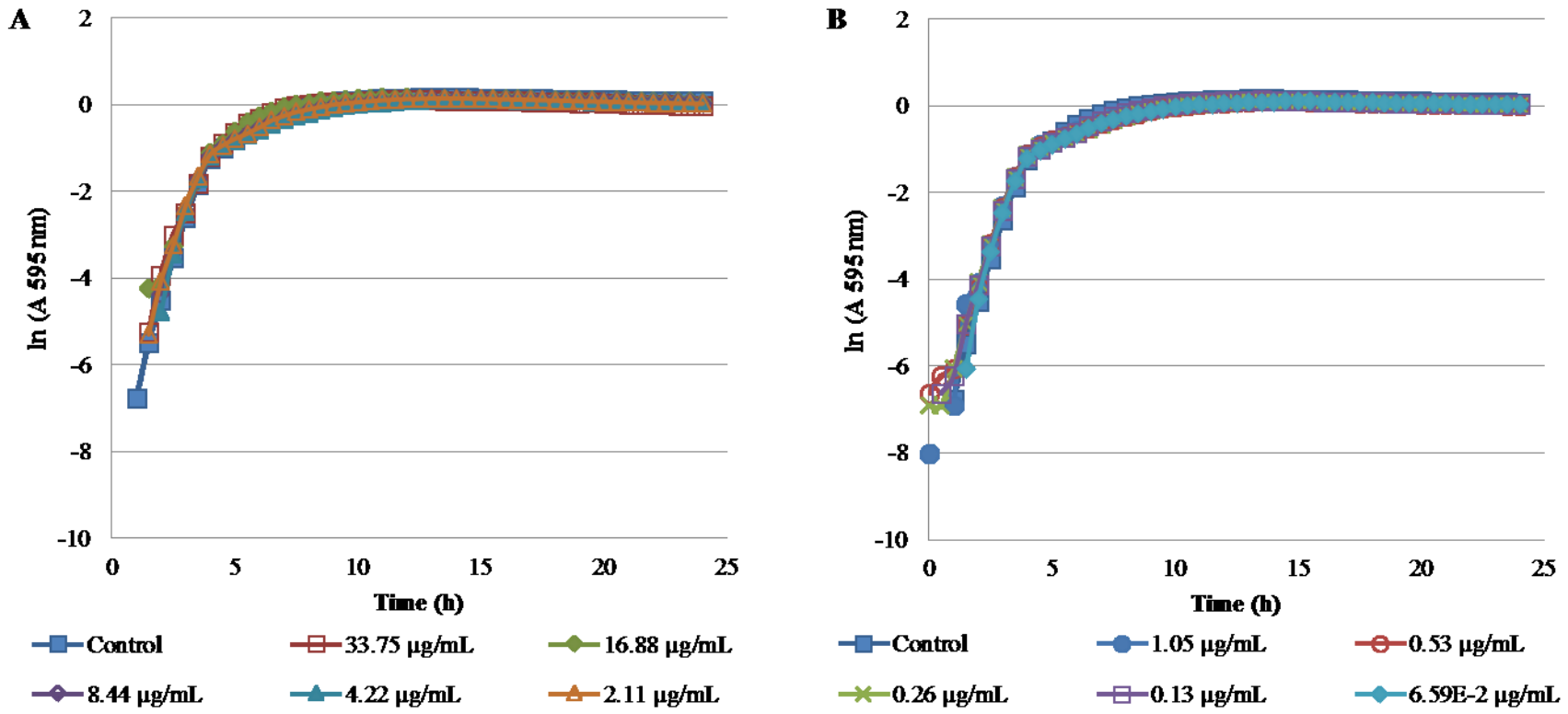

Figure 4. Growth curves of *E. coli* K12 in LB at pH 7 over a 24 hour period with aged CNTrene® C100LM treatment at and above 6.59 x 10^{-2} µg/mL. Control cells were grown in medium without CNT treatment. Wells containing growth medium and aged CNTrene® C100LM at treatment concentrations were subtracted from OD data sets in order to normalize background absorbance and distinguish bacterial growth. (A) Treated with 33.75 µg/mL, 16.88 µg/mL, 8.44 µg/mL, 4.22 µg/mL, and 2.11 µg/mL aged CNTrene® C100LM; (B) Treated with 1.05 µg/mL, 0.53 µg/mL, 0.26 µg/mL, 0.13 µg/mL, 6.59 x 10^{-2} µg/mL aged CNTrene® C100LM.

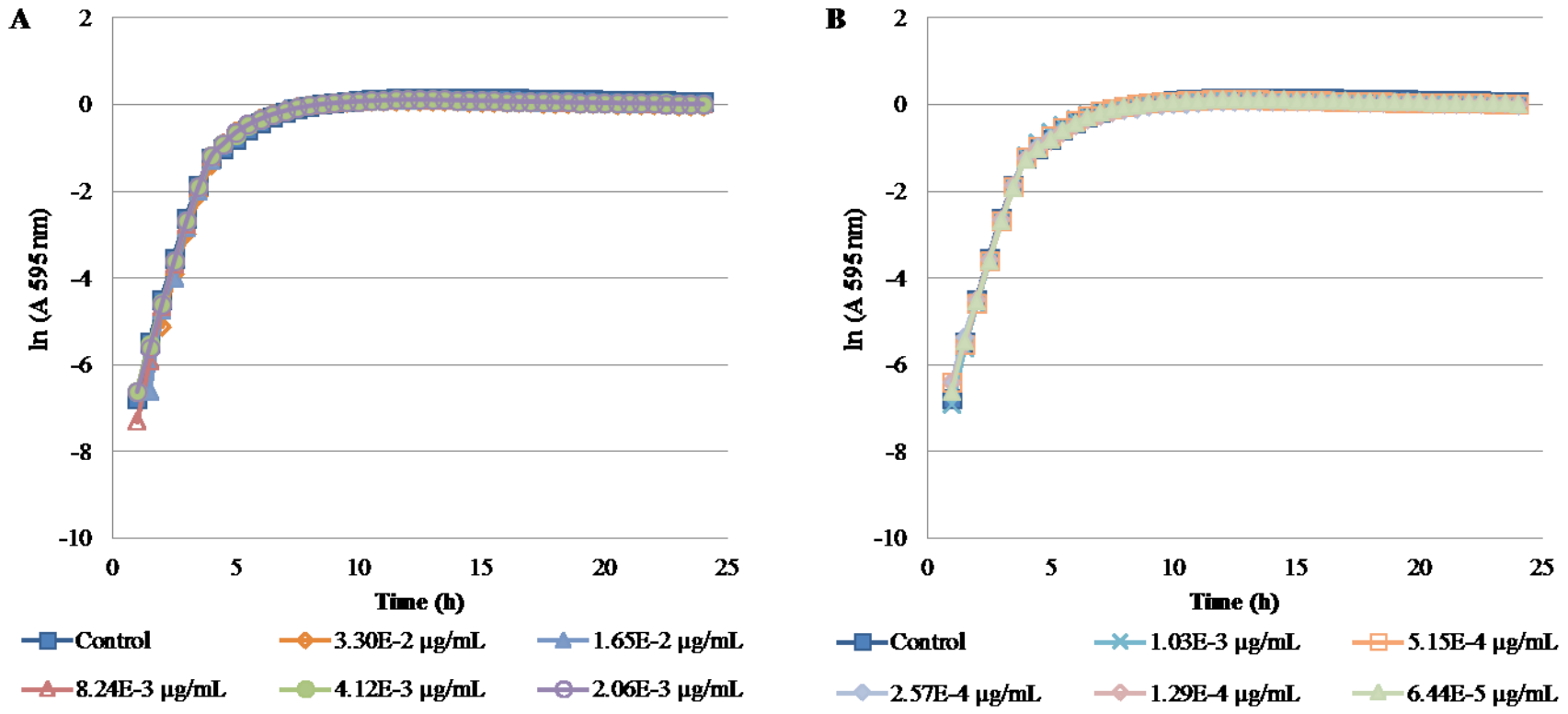

Figure 5. Growth curves of *E. coli* K12 in LB at pH 7 over a 24 hour period with aged CNTrene® C100LM treatment at and below 3.30 x 10^{-2} µg/mL. Control cells were grown in medium without CNT treatment. Wells containing growth medium and aged CNTrene® C100LM at treatment concentrations were subtracted from OD data sets in order to normalize background absorbance and distinguish bacterial growth. (A) Treated with 3.30 x 10^{-2} µg/mL, 1.65 x 10^{-2} µg/mL, 8.24 x 10^{-3} µg/mL, 4.12 x 10^{-3} µg/mL, and 2.06 x 10^{-3} µg/mL aged CNTrene® C100LM; (B) Treated with 1.03 x 10^{-3} µg/mL, 5.15 x 10^{-4} µg/mL, 2.57 x 10^{-4} µg/mL, 1.29 x 10^{-4} µg/mL, and 6.44 x 10^{-5} µg/mL aged CNTrene® C100LM.

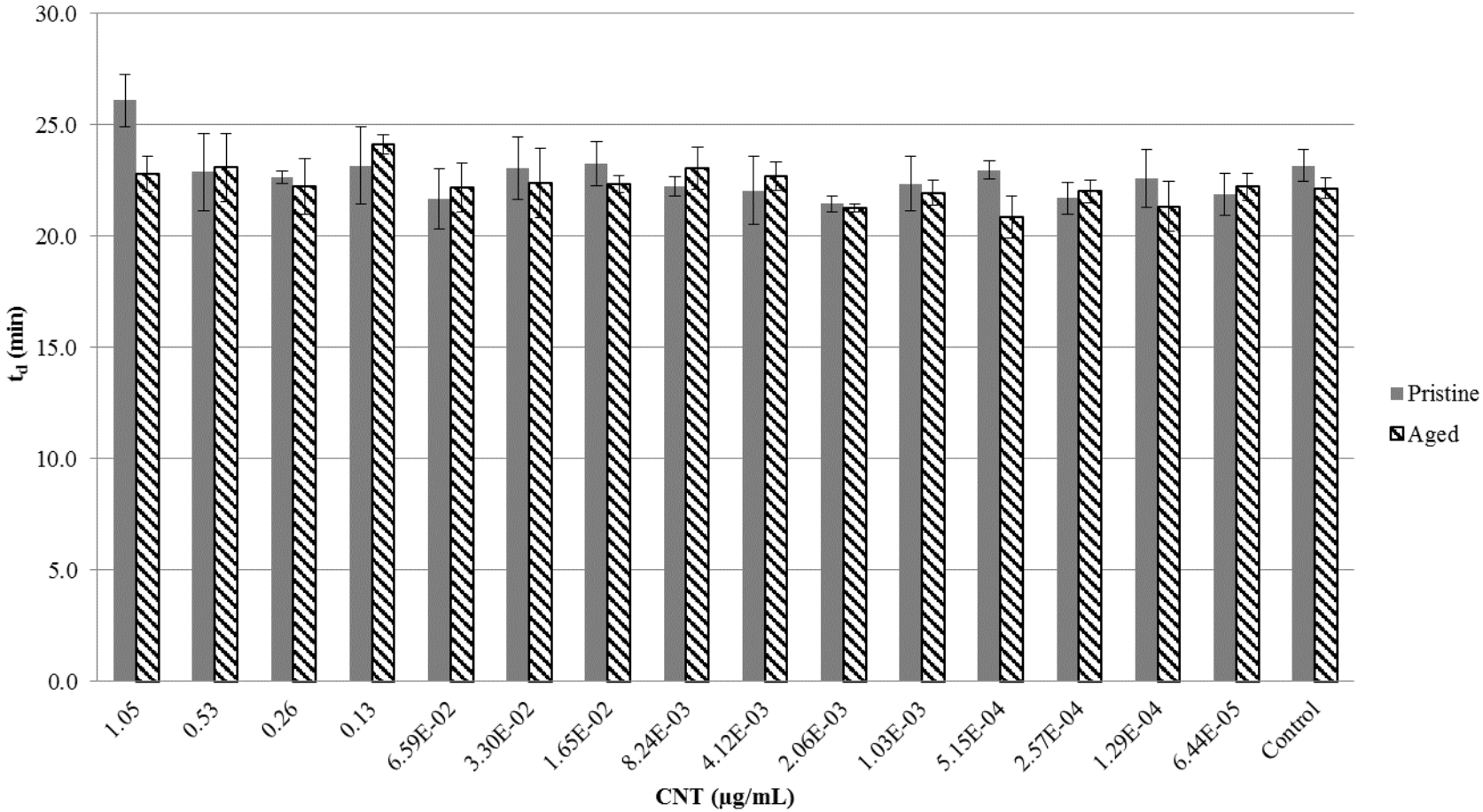

Figure 6. Comparison of doubling times (t_d) of *E. coli* K12 in LB at pH 7. Treatment with either pristine (gray bar) or artificially aged (hashed bar) CNTrene® C100LM. Controls were cells in growth medium without CNTrene® treatment. For pristine CNTrene® C100LM treatment t_d ranged from 21.4 to 26.1 min (standard deviation (sd ≤ 1.7 min); for aged CNTrene® C100LM treatment t_d ranged from 20.9 to 24.1 min (sd ≤ 1.6 min); for control groups for pristine and aged assays t_d was 23.2 min and 22.2 min respectively (sd ≤ 0.7 min).

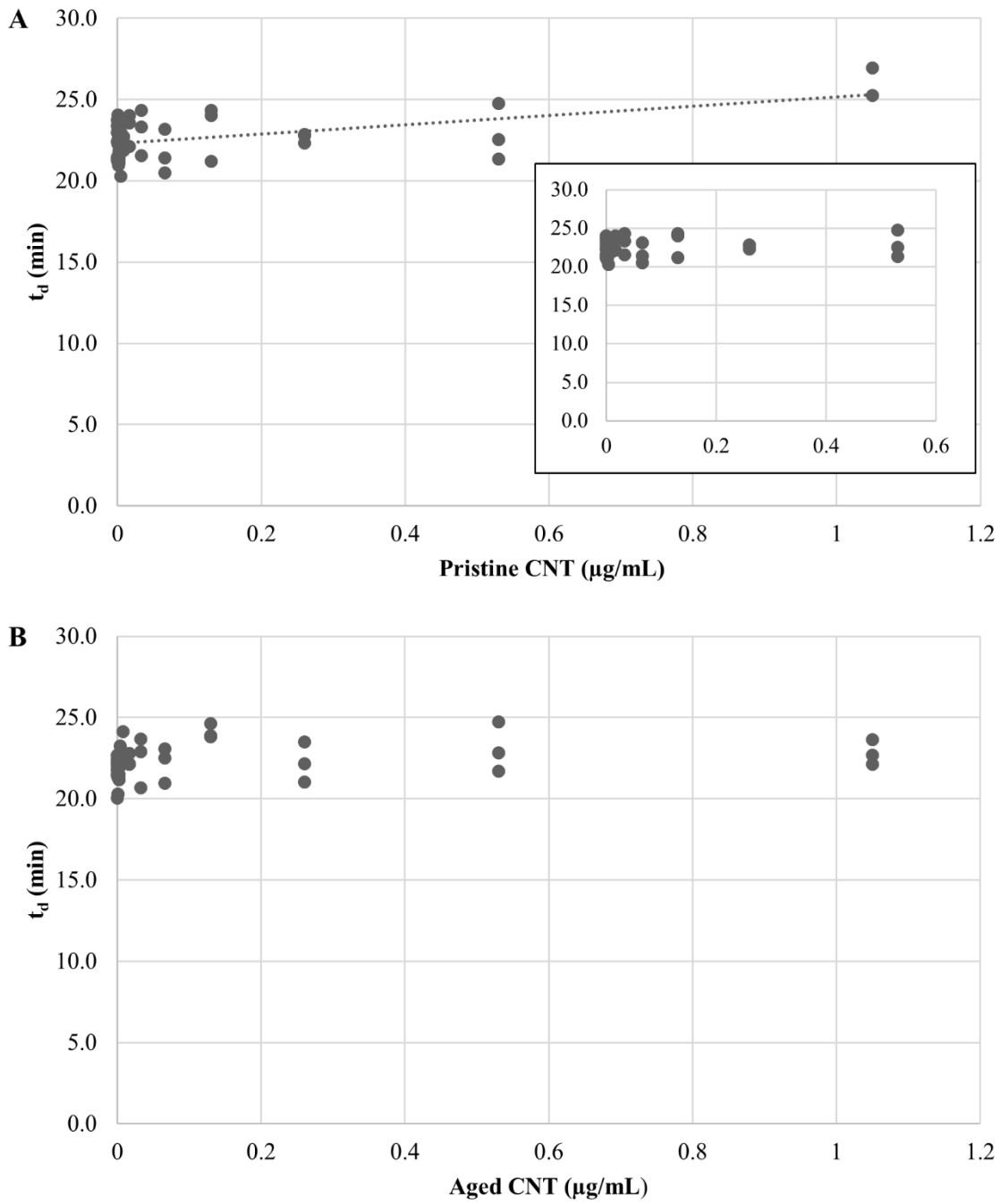

Figure 7. *E. coli* K12 doubling times at CNTrene® C100LM treatment concentrations in LB pH 7. (A) Pristine CNTrene® C100LM doubling times. Pearson correlation coefficient, $R^2 = 0.2764$; significant moderate positive correlation ($p = 0.000148$). Inset, identical data omitting the 1.05 µg/mL CNT concentration. Pearson correlation coefficient, $R^2 = 0.0197$; correlation is not significant ($p = 0.357281$). (B) Aged CNTrene® C100LM and doubling times. Pearson correlation coefficient, $R^2 = 0.0647$; correlation is not significant ($p = 0.081$).

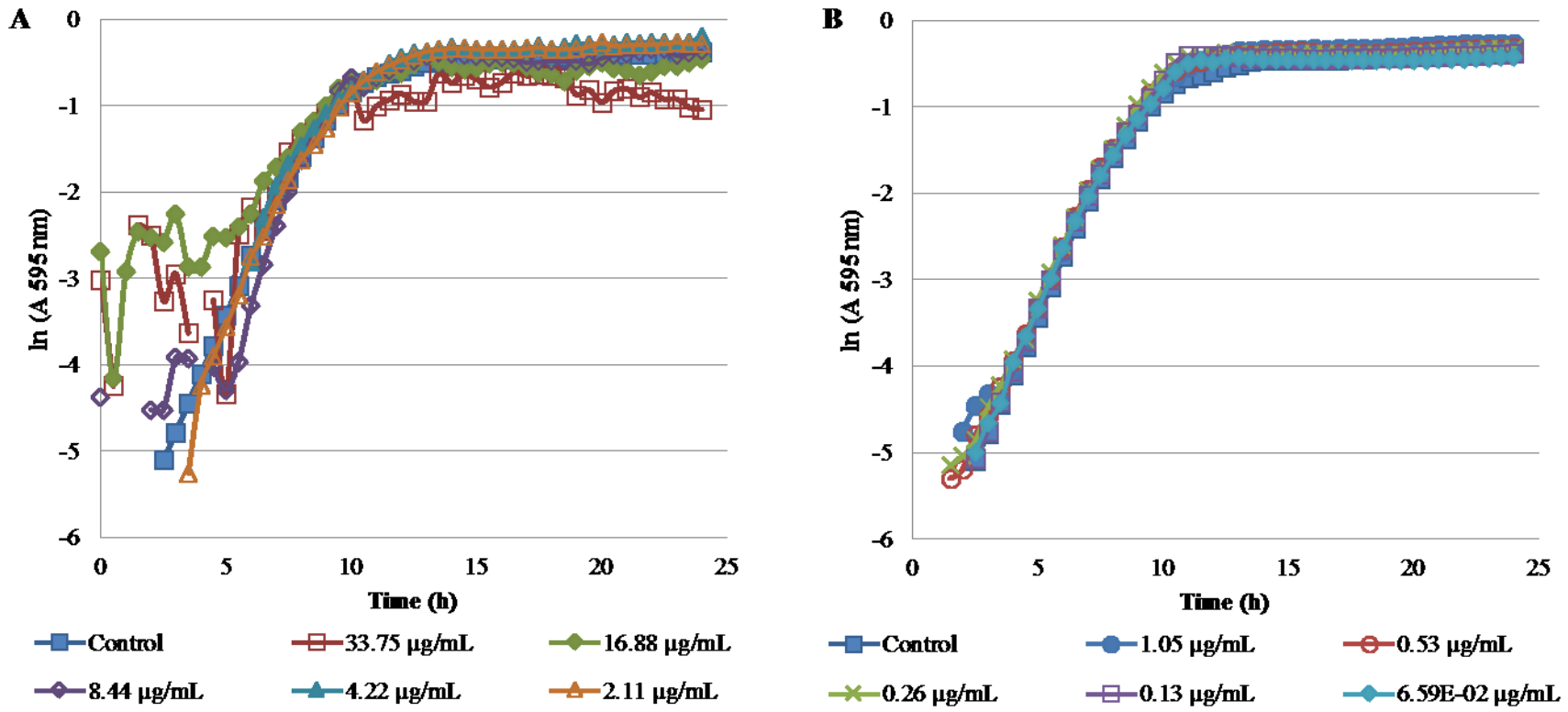

Figure 8. Growth curves of *E. coli* K12 in M9+B1 over a 24 hour period with pristine CNTrene® C100LM treatment at and above 6.59 x 10^{-2} µg/mL. Control cells were grown in medium without CNT treatment. Wells containing growth medium and pristine CNTrene® C100LM at treatment concentrations were subtracted from OD data sets in order to normalize background absorbance and distinguish bacterial growth. (A) Treated with 33.75 µg/mL, 16.88 µg/mL, 8.44 µg/mL, 4.22 µg/mL, and 2.11 µg/mL pristine CNTrene® C100LM; (B) Treated with 1.05 µg/mL, 0.53 µg/mL, 0.26 µg/mL, 0.13 µg/mL, 6.59 x 10^{-2} µg/mL pristine CNTrene® C100LM.

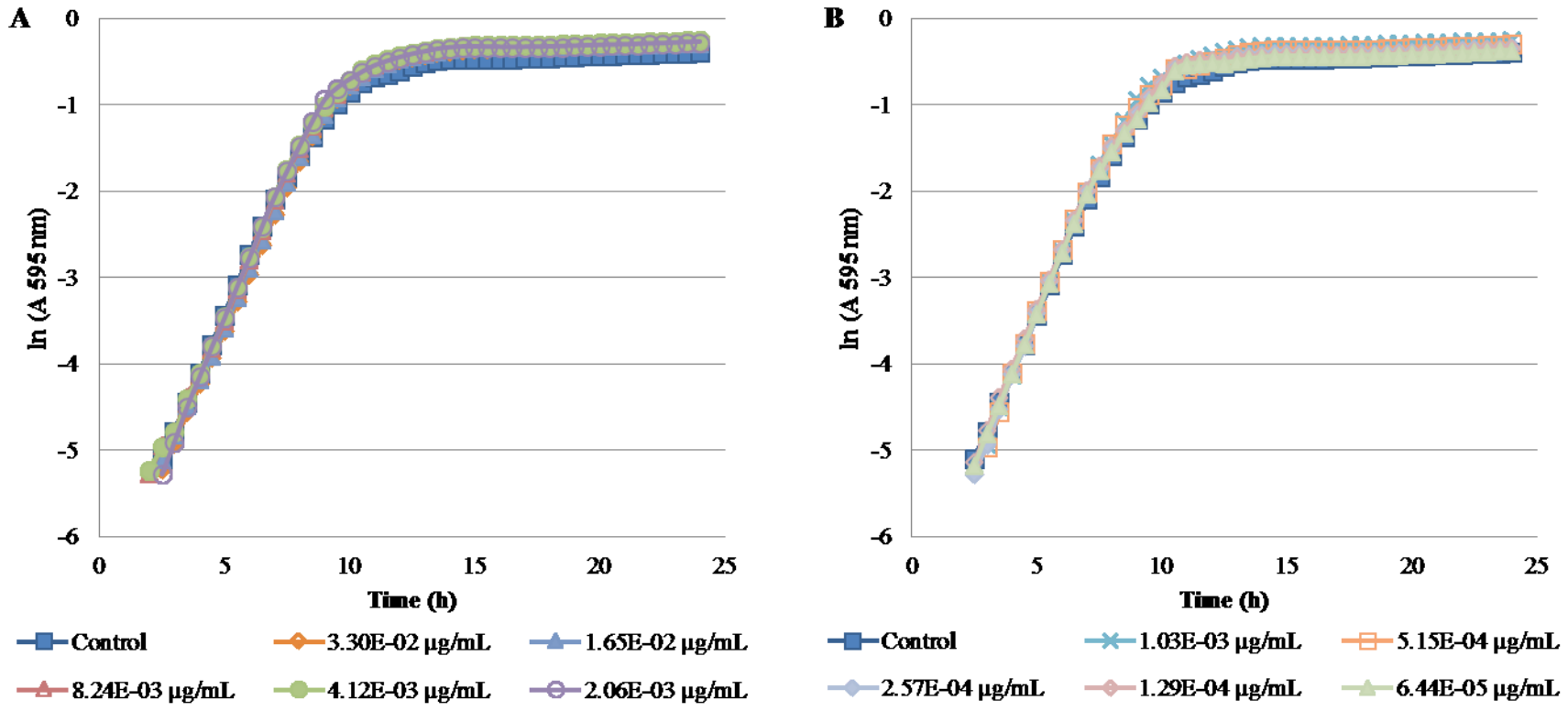

Figure 9. Growth curves of *E. coli* K12 in M9+B1 over a 24 hour period with pristine CNTrene® C100LM treatment at and below 3.30 x 10^{-2} µg/mL. Control cells were grown in medium without CNT treatment. Wells containing growth medium and pristine CNTrene® C100LM at treatment concentrations were subtracted from OD data sets in order to normalize background absorbance and distinguish bacterial growth. (A) Treated with 3.30 x 10^{-2} µg/mL, 1.65 x 10^{-2} µg/mL, 8.24 x 10^{-3} µg/mL, 4.12 x 10^{-3} µg/mL, and 2.06 x 10^{-3} µg/mL pristine CNTrene® C100LM; (B) Treated with 1.03 x 10^{-3} µg/mL, 5.15 x 10^{-4} µg/mL, 2.57 x 10^{-4} µg/mL, 1.29 x 10^{-4} µg/mL, and 6.44 x 10^{-5} µg/mL pristine CNTrene® C100LM.

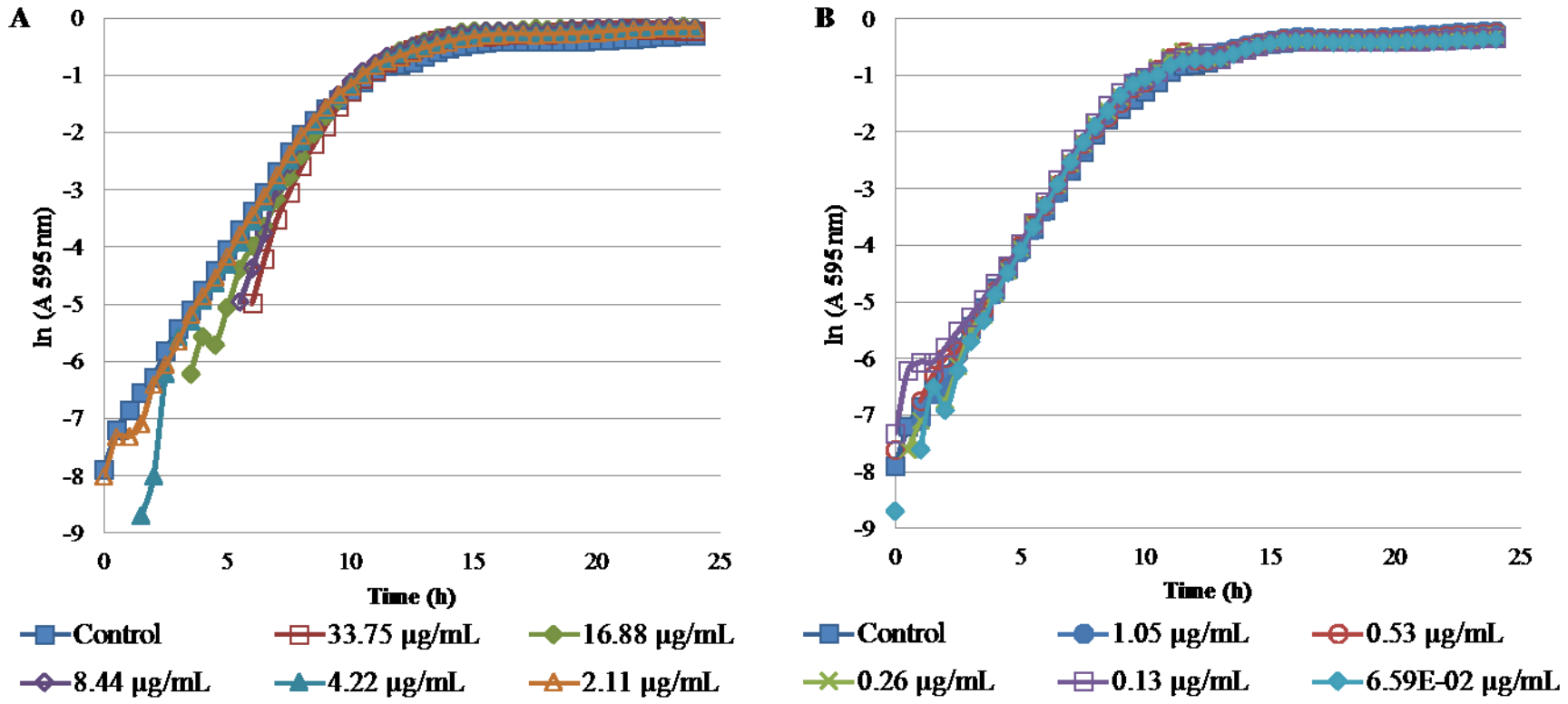

Figure 10. Growth curves of *E. coli* K12 in M9+B1 over a 24 hour period with aged CNTrene® C100LM treatment at and above 6.59 x 10^{-2} µg/mL. Control cells were grown in medium without CNT treatment. Wells containing growth medium and aged CNTrene® C100LM at treatment concentrations were subtracted from OD data sets in order to normalize background absorbance and distinguish bacterial growth. (A) Treated with 33.75 µg/mL, 16.88 µg/mL, 8.44 µg/mL, 4.22 µg/mL, and 2.11 µg/mL aged CNTrene® C100LM; (B) Treated with 1.05 µg/mL, 0.53 µg/mL, 0.26 µg/mL, 0.13 µg/mL, 6.59 x 10^{-2} µg/mL aged CNTrene® C100LM.

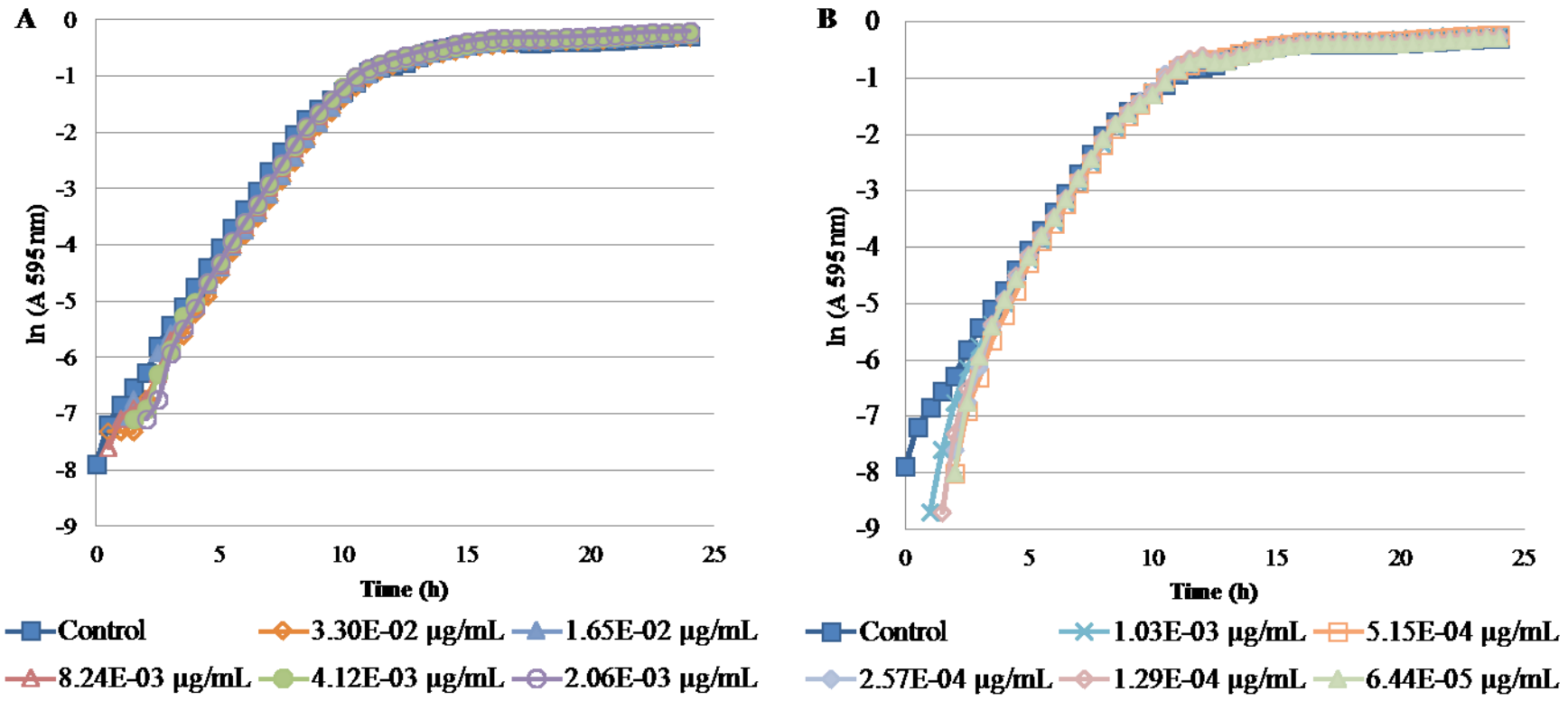

Figure 11. Growth curves of *E. coli* K12 in M9+B1 over a 24 hour period with aged CNTrene® C100LM treatment at and below 3.30 x 10^{-2} µg/mL. Control cells were grown in medium without CNT treatment. Wells containing growth medium and aged CNTrene® C100LM at treatment concentrations were subtracted from OD data sets in order to normalize background absorbance and distinguish bacterial growth. (A) Treated with 3.30 x 10^{-2} µg/mL, 1.65 x 10^{-2} µg/mL, 8.24 x 10^{-3} µg/mL, 4.12 x 10^{-3} µg/mL, and 2.06 x 10^{-3} µg/mL aged CNTrene® C100LM; (B) Treated with 1.03 x 10^{-3} µg/mL, 5.15 x 10^{-4} µg/mL, 2.57 x 10^{-4} µg/mL, 1.29 x 10^{-4} µg/mL, and 6.44 x 10^{-5} µg/mL aged CNTrene® C100LM.

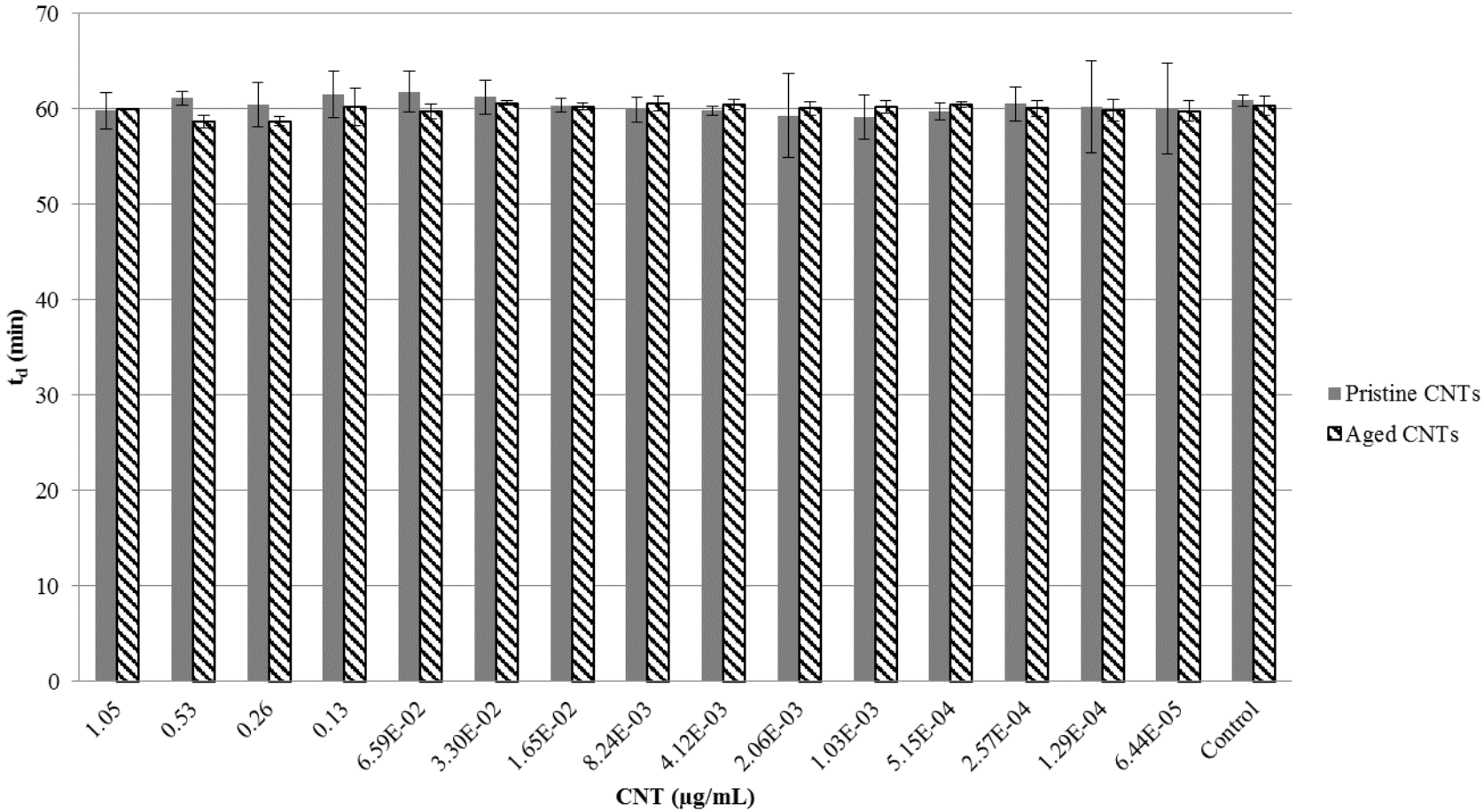

Figure 12. Comparison of doubling times (t_d) of *E. coli* K12 in M9+B1. Treatment with either pristine (gray bar) or artificially aged (hashed bar) CNTrene® C100LM. Controls were cells in growth medium without CNTrene® C100LM treatment. For pristine CNTrene® treatment t_d ranged from 59.2 to 61.8 min (standard deviation (sd) ≤ 4.9 min); for aged CNTrene® C100LM treatment t_d ranged from 58.7 to 60.6 min (sd ≤ 2.0 min); for control groups for pristine and aged assays t_d was 60.9 min and 60.3 min respectively (sd ≤ 1.0 min).

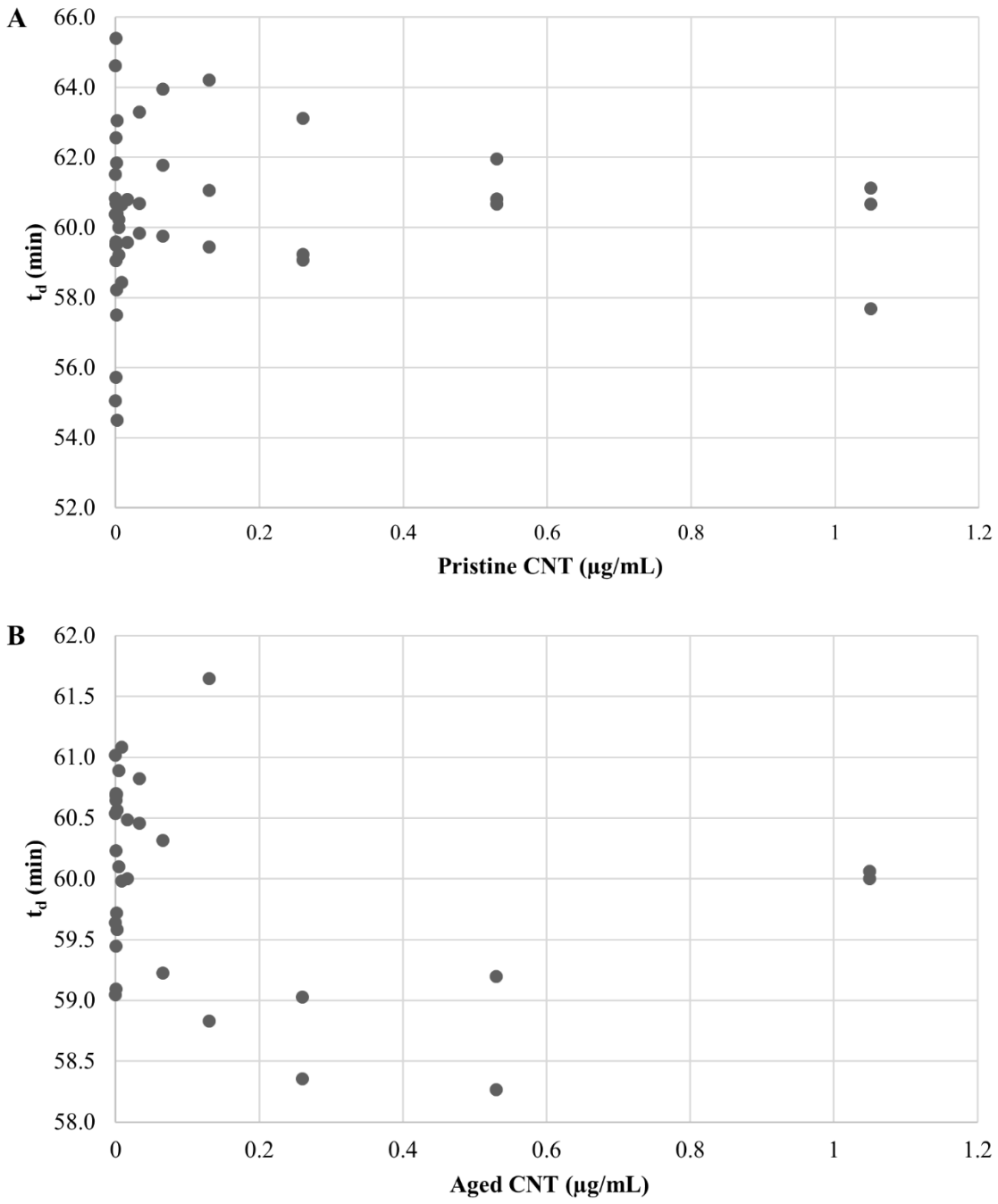

Figure 13. *E. coli* K12 doubling times at CNTrene® C100LM treatment concentrations in M9+B1. (A) Pristine CNTrene® C100LM doubling times. Pearson correlation coefficient, $R^2 = 0.0001$; correlation is not significant ($p = 0.941385$). (B) Aged CNTrene® C100LM and doubling times. Pearson correlation coefficient, $R^2 = 0.0723$; correlation is not significant ($p = 0.138074$).

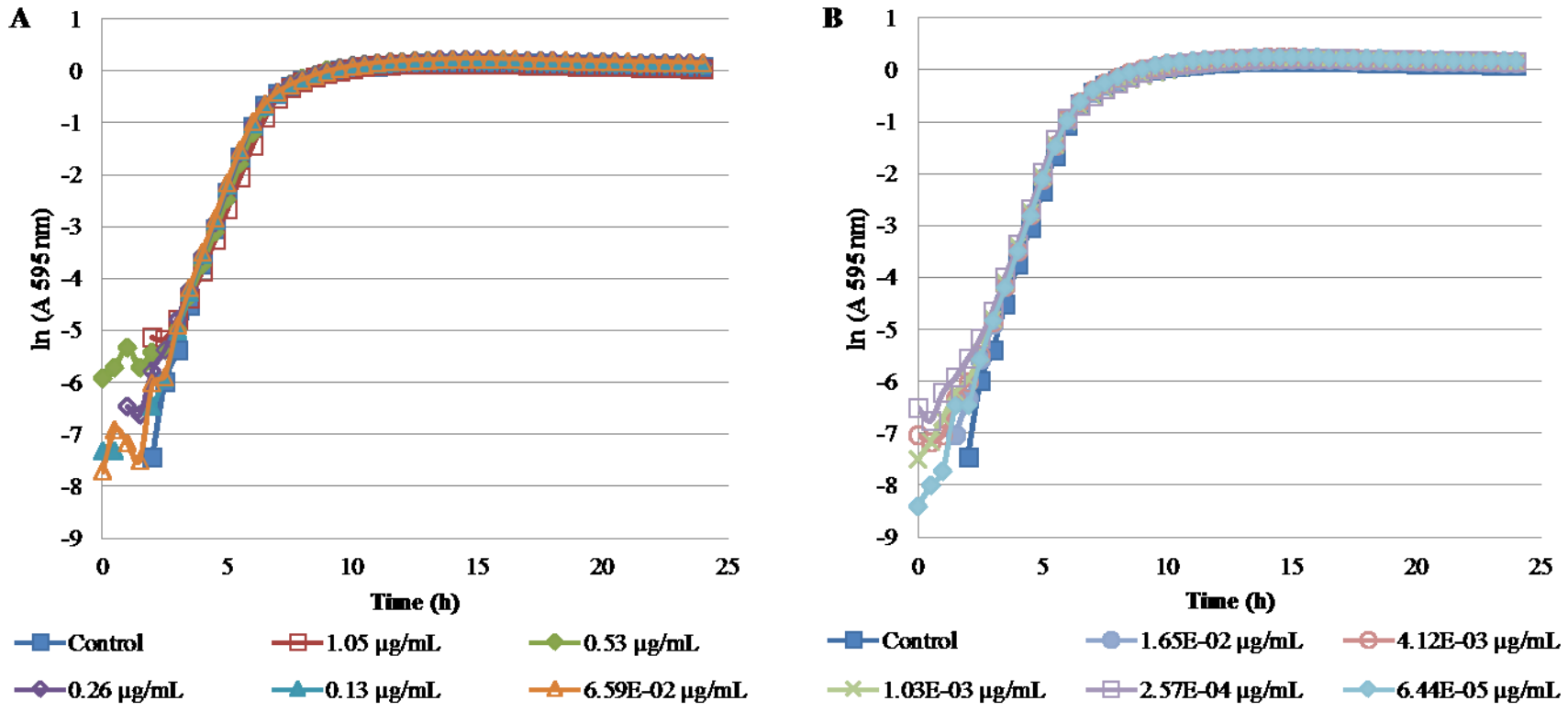

Figure 14. Growth curves of *E. coli* K12 in LB at pH 5 over a 24 hour period with pristine CNTrene® C100LM treatment. Control cells were grown in medium without CNT treatment. Wells containing growth medium and pristine CNTrene® C100LM at treatment concentrations were subtracted from OD data sets in order to normalize background absorbance and distinguish bacterial growth. (A) Treated with 1.05 µg/mL, 0.53 µg/mL, 0.26 µg/mL, 0.13 µg/mL, and 6.59 x 10^{-2} µg/mL pristine CNTrene® C100LM; (B) Treated with 1.65 x 10^{-2} µg/mL, 4.12 x 10^{-3} µg/mL, 1.03 x 10^{-3} µg/mL, 2.57 x 10^{-4} µg/mL, and 6.44 x 10^{-5} µg/mL pristine CNTrene® C100LM.

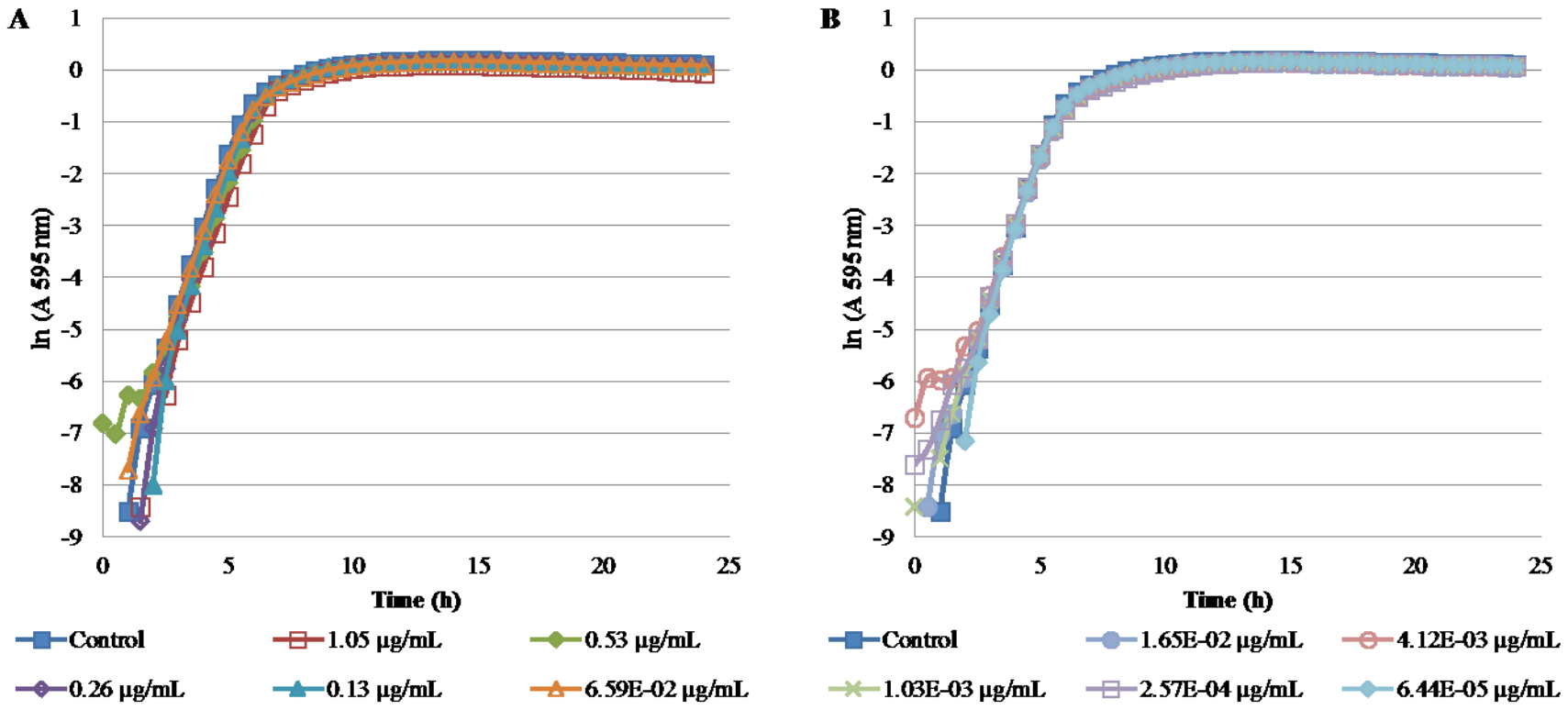

Figure 15. Growth curves of *E. coli* K12 in LB at pH 5 over a 24 hour period with aged CNTrene® C100LM treatment. Control cells were grown in medium without CNT treatment. Wells containing growth medium aged CNTrene® C100LM at treatment concentrations were subtracted from OD data sets in order to normalize background absorbance and distinguish bacterial growth. (A) Treated with 1.05 µg/mL, 0.53 µg/mL, 0.26 µg/mL, 0.13 µg/mL, and 6.59 x 10^{-2} µg/mL aged CNTrene® C100LM; (B) Treated with 1.65 x 10^{-2} µg/mL, 4.12 x 10^{-3} µg/mL, 1.03 x 10^{-3} µg/mL, 2.57 x 10^{-4} µg/mL, and 6.44 x 10^{-5} µg/mL aged CNTrene® C100LM.

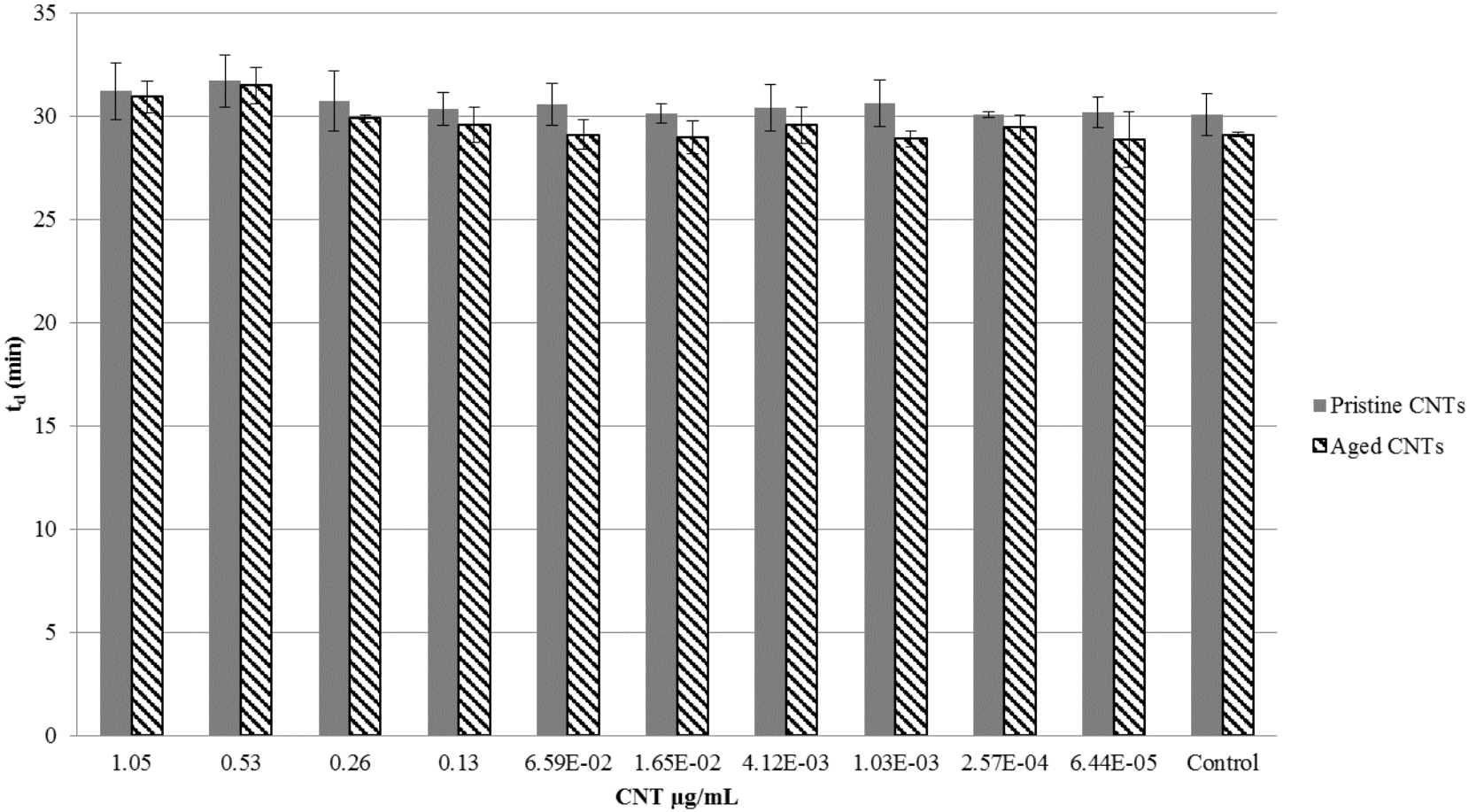

Figure 16. Comparison of doubling times (t_d) of *E. coli* K12 in LB at pH 5**.** Treatment with either pristine (gray bar) or artificially aged (hashed bar) CNTrene® C100LM. Controls were cells in growth medium without CNTrene® C100LM treatment. For pristine CNTrene® treatment t_d ranged from 30.1 to 31.7 min (standard deviation (sd ≤ 1.5 min); for aged CNTrene® C100LM treatment t_d ranged from 28.9 to 31.5 min (sd ≤ 1.3 min); for control groups for pristine and aged assays t_d was 30.1 min (sd = 1.0 min) and 29.1 min (sd = 0.1 min) respectively.

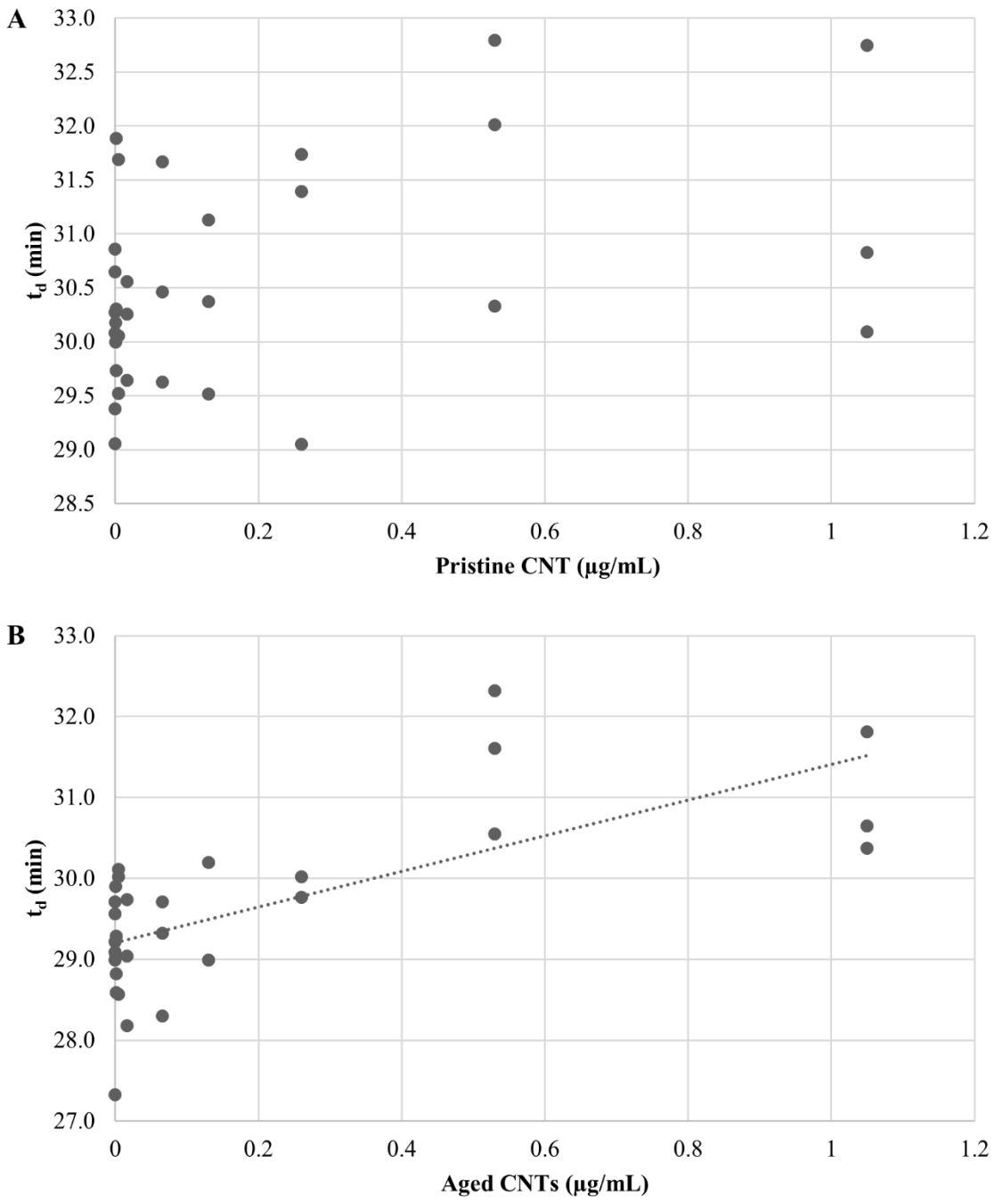

Figure 17. *E. coli* K12 doubling times at CNTrene® C100LM treatment concentrations in LB pH 5. (A) Pristine CNTrene® C100LM doubling times. Pearson correlation coefficient, $R^2 = 0.1574$; correlation is not significant ($p = 0.024581$). (B) Aged CNTrene® C100LM and doubling times. Pearson correlation coefficient, $R^2 = 0.6839$; significant moderate positive correlation ($p = 0.000031$).

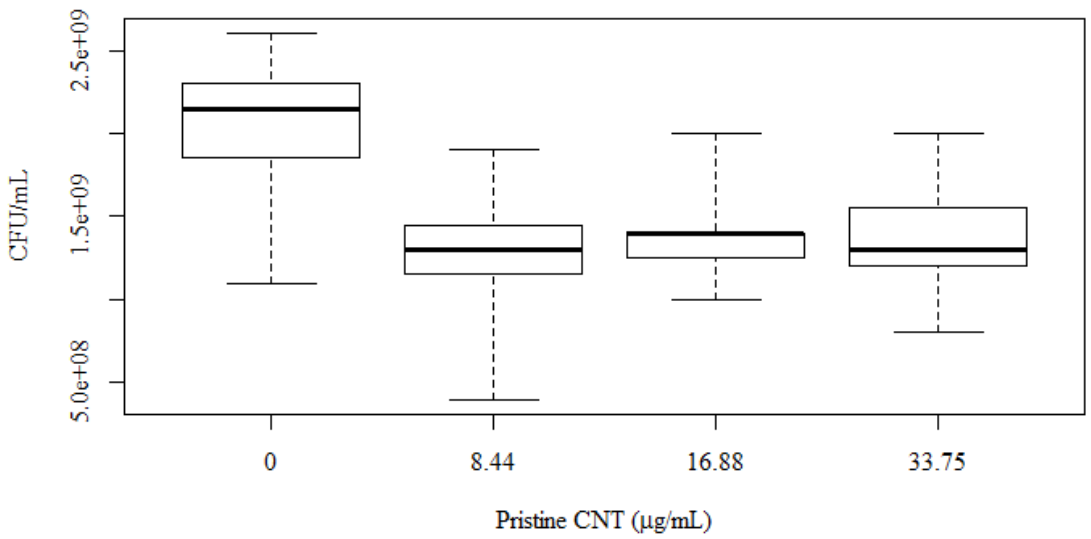

Figure 18. Comparison of colony forming units per mL (CFU/mL) for *E. coli* K12 after 24 hour exposure to pristine CNTrene® C100LM at 0 µg/mL (control), 8.44 µg/mL, 16.88 µg/mL, and 33.75 µg/mL. Each treatment group was compared to the control by unpaired t-test (two-tailed p value, 95% confidence levels) and each treatment was found to be statistically different from the control ($p = 0.0008$, $p = 0.0045$ and $p = 0.0021$ respectively). A linear regression does not significantly deviate from zero ($p = 0.4031$).

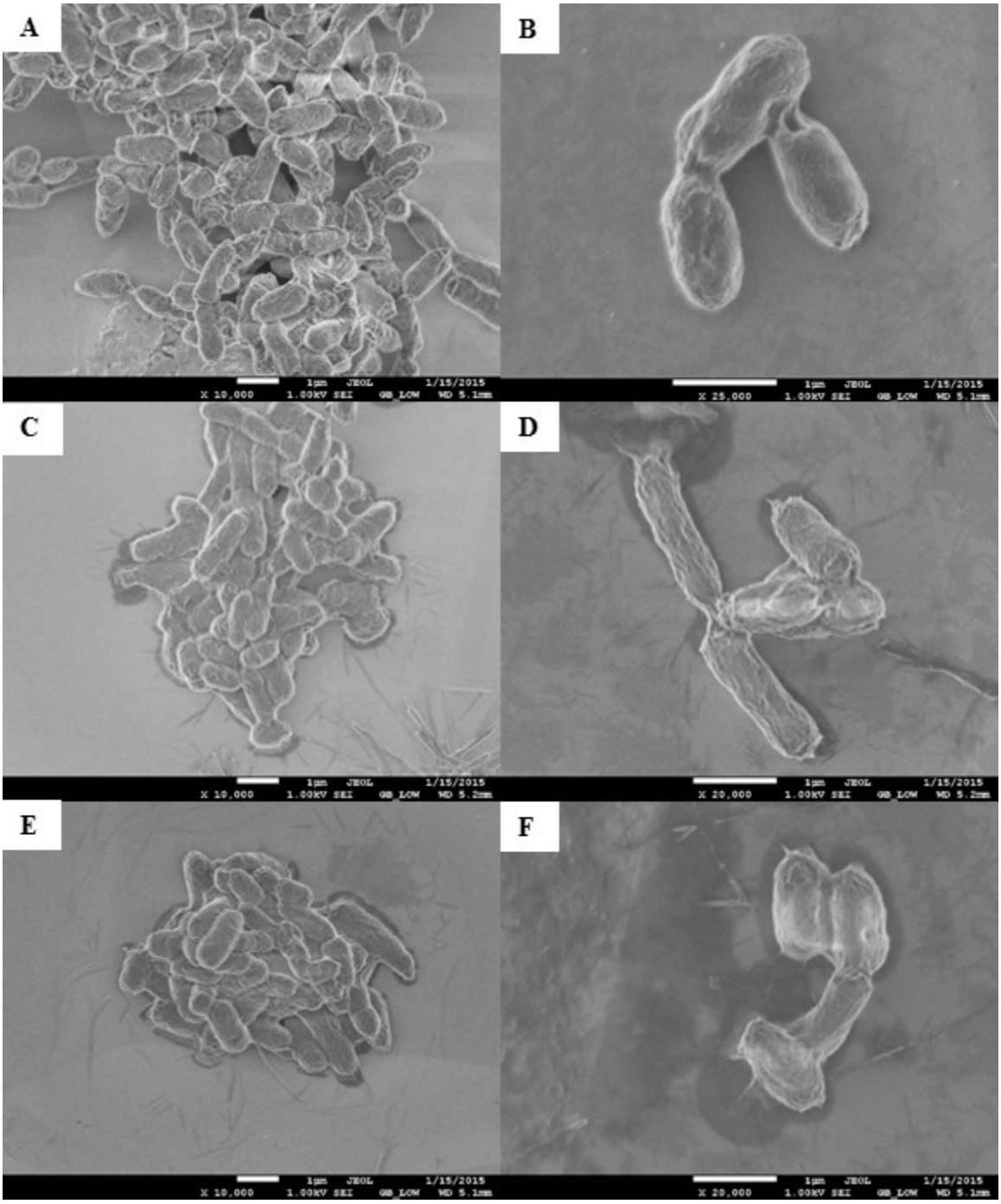

Figure 19. Scanning electron microscopy (SEM) images of *E. coli* K12 after 24 hour exposure to pristine CNTrene® C100LM. Images from JEOL JSM-7600F field emission SEM under vacuum (9.6 x 10^{-5} Pascal) with accelerating voltage of 1.00 kV. The scale bar is 1 µm. (A-B) 0 µg/mL (control), (C-D) 16.88 µg/mL, (E-F) 33.75 µg/mL pristine CNT exposure. Total magnification was 10,000x (A, C, E), 25,000x (B), and 20,000x (D, F).

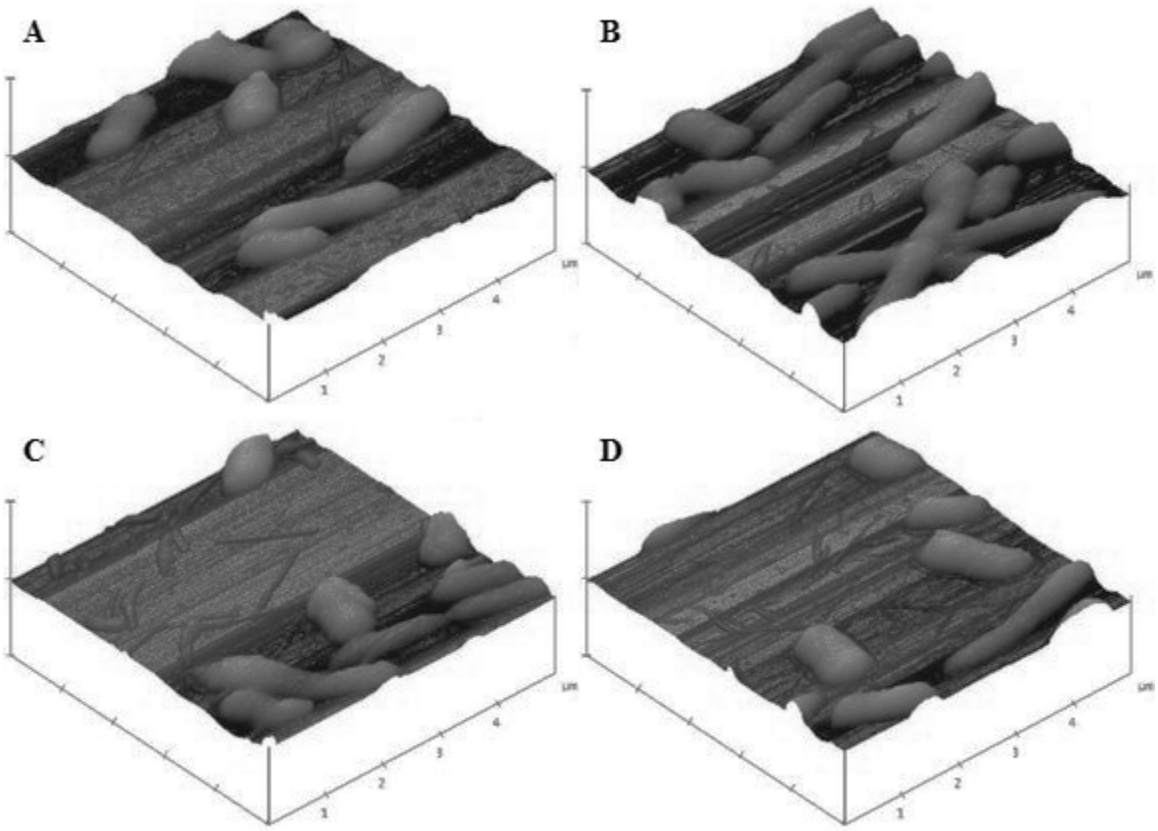

Figure 20. Atomic force microscopy (AFM) images of *E. coli* K12 after 24 hour exposure to pristine CNTrene® C100LM using a 5.000 µm scan size**.** Three dimensional images from Veeco Dimension 3100 with a Nanoscope IIIA Controller using tapping mode and a silicon tip (radius of 8.0 nm) under atmospheric conditions. All images captured with a scan rate of 1.001 Hz and 512 samples. Data scale for all images was 2.000 µm with X position of -19783.4 µm and Y position of -42151.3 µm. (A) 0 µg/mL (control), (B) 1.05 µg/mL, (C) 16.88 µg/mL, (D) 33.75 µg/mL pristine CNT exposure.

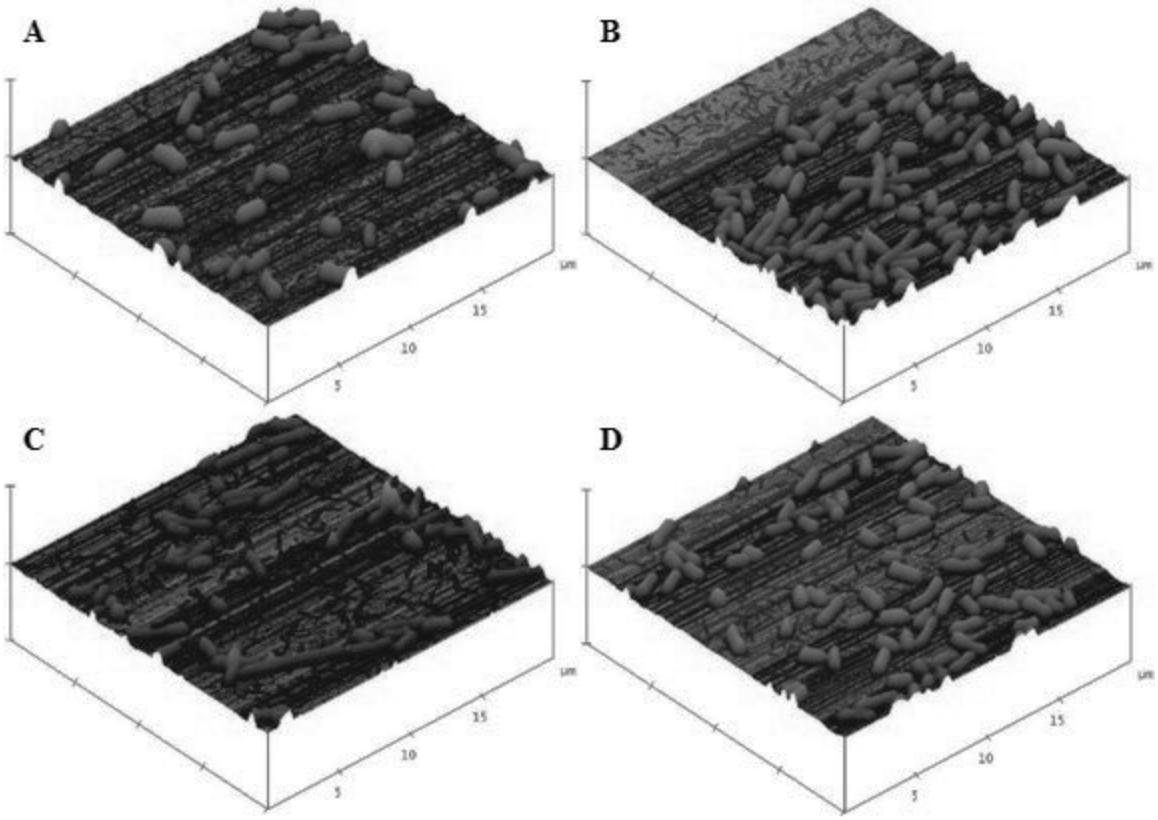

Figure 21. Atomic force microscopy (AFM) images of *E. coli* K12 after 24 hour exposure to pristine CNTrene® C100LM using a 20.00 µm scan size. Three dimensional images from Veeco Dimension 3100 with a Nanoscope IIIA Controller using tapping mode and a silicon tip (radius of 8.0 nm) under atmospheric conditions. All images captured with a scan rate of 1.001 Hz and 512 samples. Data scale for all images was 3.000 µm with X position of -19783.4 µm and Y position of -42151.3 µm. (A) 0 µg/mL (control), (B) 1.05 µg/mL, (C) 16.88 µg/mL, (D) 33.75 µg/mL pristine CNT exposure.

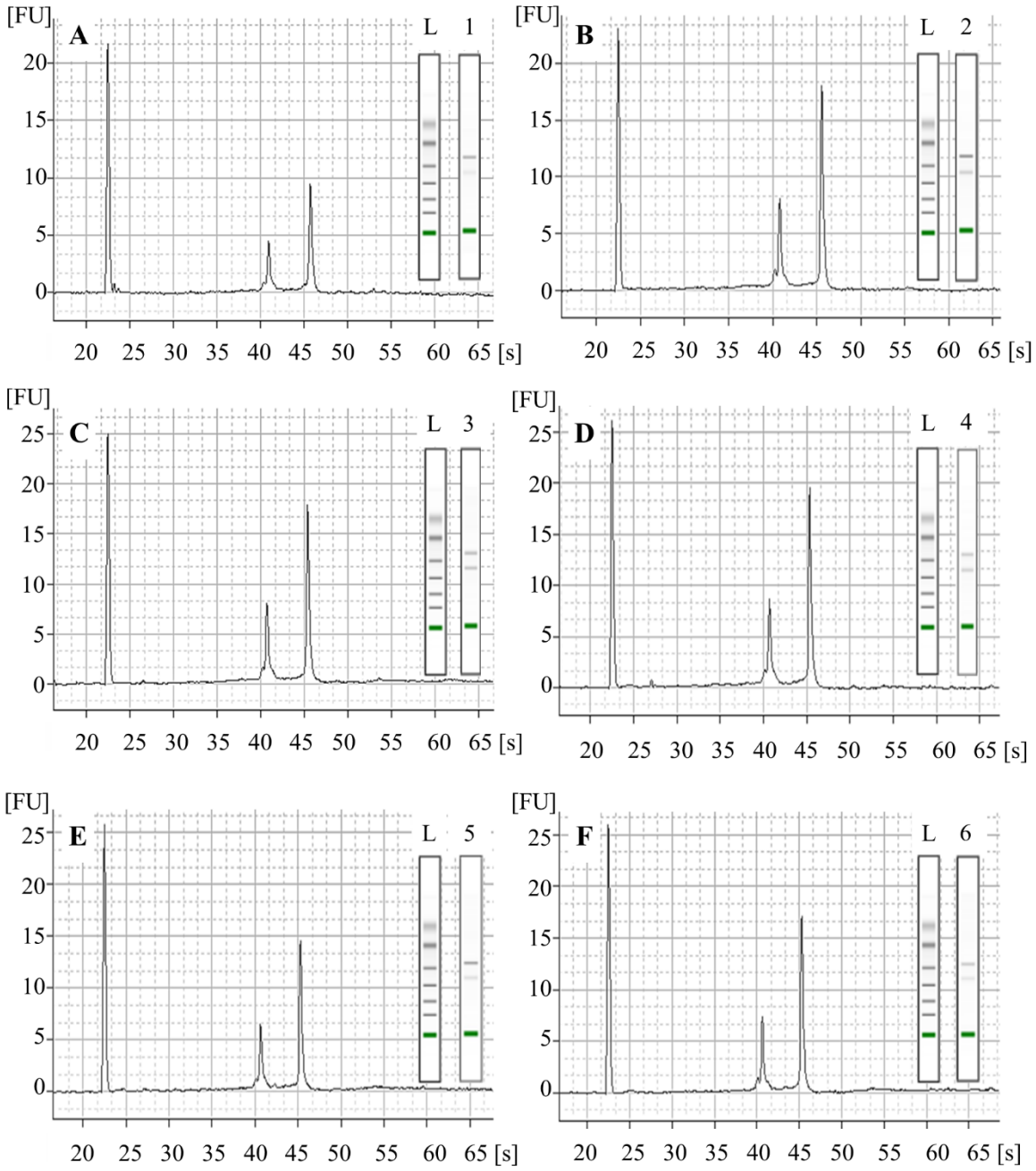

Figure 22. Electropherograms and simulated gel images for total RNA samples extracted from *E.coli* K12 cultures. Electropherograms and simulated gel images from Agilent Technologies 2100 Bioanalyzer system using 2100 Expert software. Simulated gel image of RNA ladder (L) [From top: 4000 nucleotides (nt), 2000 nt, 1000 nt, 500 nt, 200 nt, and 25 nt] included for comparison to sample lanes (insets). Electropherograms illustrate fluorescence units (FU) against time in seconds for: (A) Control sample 1; (B) Control sample 2; (C) Control sample 3; (D) Pristine CNTrene® treatment (1.05 µg/mL) sample 1; (E) Pristine CNTrene® C100LM treatment (1.05 µg/mL) sample 2; (F) Pristine CNTrene® C100LM treatment (1.05 µg/mL) sample 3.

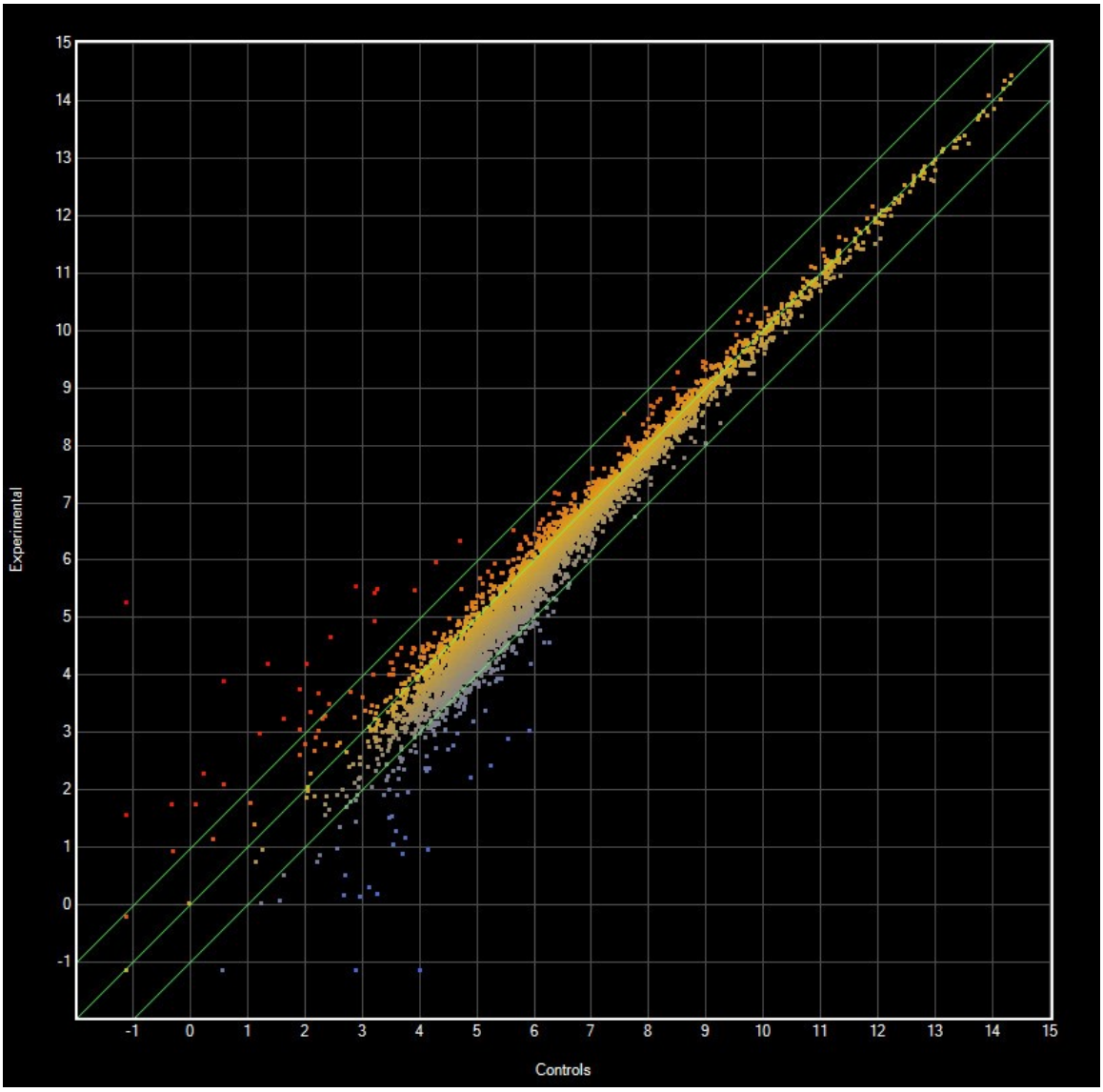

Figure 23. Comparison of median gene expression in control and experimental data sets. Twenty six genes were ≥ 2-fold upregulated in CNT exposed cells, while 160 genes were ≥ 2-fold downregulated in CNT exposed cell and 4128 genes did not have differential expression ($R^2 = 0.9643$).

4 DISCUSSION

4.1 Importance of Evaluation for CNT Products and Technology

With the emergence of nanotechnology and the growing number of applications for carbon nanotubes, such as biosensors (Chen et al 2003; Wang et al. 2003; Yun et al 2007; Huang et al. 2004; Timur et al 2007; Trojanowicz et al 2006) and vaccine/drug delivery systems (Bianco et al. 2005; Cai et al. 2005; Liu et al. 2007; Kam et al. 2005), it is important that the safety and potential impacts of nanoparticles on human health and environmental communities are fully evaluated. The potential cytotoxic effects on microbial communities is an important consideration during a chemical life cycle analysis, as these organisms play a vital role in environmental nutrient cycling, are essential for the maintenance of animal life, and play a role in health and disease. Consequently, disruption of the microbiota of an ecosystem has wide reaching consequences.

4.2 MIC and Non-Lethal Effects

In this study, the growth of *E. coli* K12 was not completely inhibited by either pristine or aged CNTrene® C100LM over the tested concentration range of 6.44×10^{-5} µg/mL to 33.75 µg/mL under any of the growth conditions tested. Therefore, a MIC value after treatment with either pristine or aged CNTs was not observed. Growth curves for both pristine and aged CNTs overlaid with the corresponding controls without CNT exposure at all tested concentrations, regardless of media composition used. These data suggest that CNTrene® C100LM had no observable lethal or non-lethal effect on *E. coli*

K12 growth. Concentrations of CNTs greater than 1.05 µg/mL had a high initial optical density due to background interference from the black CNT solution, which made finding a linear portion of the growth curve difficult for determination of doubling time. Therefore, doubling times with CNT concentrations great than 1.05 µg/mL were not reliable and plate counts were used to determine viability. Using plate counts, the cytotoxicity of concentrations of pristine CNTrene® between 8.44 µg/mL – 33.75 µg/mL was evaluated via a modified spot plate technique (Gaudy et. al., 1963). Although the cell number in CNT exposed cells appeared to be slightly lower than unexposed cells (t-test, $p < 0.05$), the difference in cell number was less than or equal to a 1.61-fold reduction in CFU/mL compared to the control at all CNT exposure concentrations. Moreover, a regression analysis suggests that these data do not significantly deviate from a slope of zero ($p = 0.4031$). These data imply that a there is no true biological difference in the slight reduction in CFU/mL when *E. coli* is exposed to up to 33.75 µg/mL CNTs.

In addition to antibacterial plate counts, non-lethal growth effects of pristine CNTrene® C100LM at concentrations at and above 1.05 µg/mL were evaluated by electron microscopy. It is important to mention that during sample preparation, specifically the ethanol wash series, there was potential for losing small amounts of CNTs in the supernatant which could reduce the concentration of CNTs that were observed during visualization. Additionally, CNTs could be mechanically separated from the cell surface during centrifugation, despite the low g-force used to pellet the cells. This could also contribute to a reduction in CNT concentration in the final preparation. Yet, electron microscopy imaging of *E. coli* K12 revealed no observable morphological change between control cells and cells after 24 hour exposure to pristine CNTrene®

C100LM at concentrations up to 33.75 µg/mL. Furthermore, *E. coli* K12 cells showed no preference for attachment or aggregation to the CNT material, despite the tendency for bacterial cells to attach to surfaces and form biofilms or to aggregate with each other (Beloin et al 2008; Imuta et al. 2008). However, it would also be expected that negatively charged carboxyl functional groups on the sidewalls of CNTs would repel the net negative charge of bacterial cells, which likely accounts for the low level of observed association between cells and CNTs. This is in agreement with studies examining the cytotoxicity of fullerenes on bacteria. Fullerenes are a related carbon nanomaterial to CNTs, consisting of a cage-like sphere of carbon boned in hexagonal or pentagonal arrangements. So, CNTs can be considered a cylindrical form of a fullerene with similar surface and atomic structure and composition. In fullerenes, cationic functionalization (e.g. $-NH_2$) is generally associated with increased cytotoxicity compared to anionic functionalization (e.g. -COOH) (Jensen et al 1996; Oberdörster etal 2005; Bosi et al 2003). It is unsurprising that a similar trend would be observed for carboxyl functionalized SWCNTs as they are quite similar to fullerenes.

The effect of pristine CNT exposure on the gene expression in *E. coli* K12 was evaluated by RNA sequencing and of the 4314 genes mapped, only three genes (*pptA, alpA,* and *mgtL*) were found to have significantly different expression levels. None of these differentially expressed genes are related to each other. It should be noted that the *pptA* gene had only a slight expression change of 2.5-fold down regulation in CNT exposed cells, just above the 2-fold change threshold. In contrast, the *alpA* and *mgtL* genes were highly differentially expressed at 35.1-fold down regulated and 85.3-fold upregulated, respectively. However, the role of these three genes is enigmatic because of

their unrelated cellular roles.

The *pptA* gene encodes a putative 4-oxalocrotonate tautomerase and is implicated in degradation pathways for xenobiotic aromatic compounds (Whitman 2002; Almrud et. al. 2002). The slight down regulation of *pptA* (2.5-fold) is curious because the natural substrate is unknown. Furthermore, other genes involved in aromatic degradation pathways (i.e. mono-oxygenases) were not differentially expressed. This low level of regulation of *pptA* and an absence of regulation in genes that contribute to related pathways implies that the observed regulation may be due to sequencing bias, and not true regulation. Therefore, these expression levels should be confirmed by an alternative method, such as qPCR.

The *alpA* gene is a regulatory gene for the cryptic prophage C4-57 and is part of the MerR superfamily of transcription regulators, which regulate in response to environmental stressors (Marchler-Bauer et al. 2015). Expression of *alpA* increases the expression of *intA*, encoding an integrase, which promotes excision of the CP4-57 cryptic prophage (Kirby et. al. 1994). Although no other genes involved in prophage maintenance were differentially expressed, the strong down regulation of *alpA* (35.1-fold) suggests that CNTrene® C100LM exposure may promote stable integration of the CP4-57 cryptic prophage in the genome of *E. coli* K12. The *alpA* gene has also been implicated in a role in biofilm formation since its expression was 6.5-fold higher in *E. coli* lacking the autoinducer-2 transporter *tqsA*, which is induced in biofilms (Herzberg et. al. 2006). The regulation of phage genes has also been implicated in biofilm formation in *Xylella fastidiosa* (de Souza et al. 2004) and *Pseudomonas aeruginosa* (Webb et al. 2003). However, the role of phage-related genes in the formation of biofilms is currently

unknown. It is interesting to speculate that the down regulation of *alpA* is involved in down regulating biofilm formation, which may explain the lack of CNT-bacteria association as observed by SEM.

The differential expression in the *mgtL* gene that acts as a Mg^{2+} porin leader sequence could serve as a potential sign of membrane stress as it acts as a riboswitch to promote Mg^{2+} uptake by promoting expression of the *mgtA* gene encoding the Mg^{2+} porin (Park et al. 2010). Although the *mgtA* leader had the highest regulation (85.3 up regulation), the transcript abundance of *mgtA* remained unchanged (1.0-fold expression change). This is likely due to the complex regulation of *mgtA* expression by both proline and Mg^{2+}. Both low proline and low Mg^{2+} concentrations are required for transcription of *mgtA* (Park et al. 2010). However, the M9+B1 medium used contains an abundant supply of Mg^{2+} (i.e. 200 mM). Consequently, it is not surprising that an increase in *mgtL* did not influence *mgtA* expression.

The lack of large changes in gene expression is not surprising given that growth was not significantly impacted by CNT exposure. However, it would be expected that gene regulation may play a role in normalizing growth behavior in CNT exposed cells. Yet, almost no gene regulation was seen and the few genes that were regulated were not differentially expressed to a large extent (i.e. > 100-fold). Interestingly, differential gene regulation has been previously reported to influence gene regulation. For example, CNT exposure to non-functionalized SWCNTs and MWCNTs was reported to activate genes associated with membrane and oxidative stress (Kang et al. 2008). Yet, no genes involved in these process were differentially expressed in CNTrene® C100LM exposed cells. Taken together, these data suggest that CNTrene® C100LM exposure does not cause cell

damage, death or influence growth. Furthermore, cells do not have a preference to adhere or associate with these CNTs, suggesting that exposure to even high levels of CNTrene® C100LM is innocuous to *E. coli* K12.

4.3 Comparison to Current Studies on SWCNTs

The findings of this study suggest exposure to the carboxyl functionalized SWCNT product CNTrene® C100LM does not negatively impact cell viability in *E. coli* K12, which is surprising given that many SWCNTs have been reported as having cytotoxic effects on various cell lines at and below treatment concentrations that were used in this study (Table 4). Current studies evaluating cytotoxic effects of CNTs on bacterial cells demonstrate the need for adequate characterization of the CNT materials tested, since physical and chemical properties of CNTs, including length, diameter, and functionalization, have shown an effect on cell viability observed in bacterial cells (Table 4). For example, CNTs with smaller diameters are generally more toxic than those with larger diameters (Kang et al 2008). Moreover, SWCNTs tend to be more toxic as their length increases (Yang et al. 2010).

The *in vitro* effects of SWCNT on human dermal fibroblasts cell lines have demonstrated that the degree of functionalization has a distinct effect on observed cytotoxicity (Sayes et al. 2006). In human dermal fibroblasts, cytotoxicity decreases as the degree of phenylated functionalization increasing (Sayes et al. 2006). Similarly, it has been reported that surface functionalization has an impact on the observed cell viability in *E. coli* K12 cultures, though the decrease in cytotoxicity with functionalization was thought to be an indirect effect due to change in aggregation size (Pasquini et al. 2012). It

should be noted that the actual concentration of SWCNT exposure to cells used by Pasquini et al. 2012 was hard to determine since SWCNTs were coated on a PTFE membrane and *E. coli* K12 cells were filter onto this membrane for attachment. This creates an artificial interaction between cells and CNTs that would not otherwise be found in natural planktonic conditions or natural biofilm formation. Furthermore, heavy metal content of CNTs used in the study is unknown as it was not reported. Antimicrobial effects of non-functionalized SWCNTs have been reported in both gram negative and gram positive model organisms, with physical piercing of cellular membranes by individually dispersed SWCNTs being the observed mechanism of cytotoxicity. The presence of trace amounts of Co metal, used as a catalyst in CNT synthesis, up to 1.0 μg/mL did not affect cytotoxicity (Liu et al. 2009). Other conditions, including surfactants used to suspend SWCNTs have also affect microbial cell viability and demonstrates that there are compounding factors when evaluating cytotoxicity of nanomaterials (Dong et al. 2011).

It should be addressed that there are many contradictory findings about cytotoxicity of SWCNTs, which have been attributed to the variety of SWCNTs available including differences in purity and heavy metal content left over from CNT production (Yang et al. 2010). While some studies have found strong cytotoxic activity with SWCNTs that have carboxyl functionalization (Arias and Yang 2009), others have reported the opposite finding (Lewinski et al. 2008). Most studies examine cytotoxicity of SWCNTs that are artificially coated onto membranes by filtering cells through the membrane. This procedure can lead to an inflated CNT exposure concentration and forces a CNT-cell interaction that may not accurately reflect planktonic bacterial

cytotoxicity or cytotoxicity in biofilms. Moreover, many cytotoxicity studies that do report CNTs as highly toxic in planktonic cell cultures only report toxicity associated with the CNT-cell aggregates (Kang et al 2008; Kang et al. 2007). This also artificially inflates toxicity because the majority of the cells are suspended and not in association with CNTs or CNT aggregates. For example, non-functionalized SWCNTs were reported to cause 80% loss of *E. coli* K12 viability in liquid cultures. However, this was only for SWCNT-bacterial aggregates, while the viability for cells in free suspension without CNT-association was only reduced by 8%. This was equivalent to the loss of viability of untreated cells (Kang et al. 2008). This suggests that a physical interaction is necessary for CNT cytotoxicity. Most cells grown in liquid culture are 'free-swimming' and not CNT-associated. Consequently, studies that only examine these associations and ignore the majority of the cells (i.e. in bulk solution) greatly overestimate the cytotoxic effect of the CNT in question. Due to the variation in reported effects and the variety of potential applications, it is imperative that the effects of each distinctive type of CNT and their characterization is adequately evaluated using standardized methods to obtain a clear picture of toxicity.

4.4 Future Direction in Evaluating Bacterial Cytotoxicity of Nanoparticles

This study included the use of RNA sequencing which compared the gene expression of *E. coli* K12 exposed to pristine CNTrene® C100LM to native gene expression. Future works for this study would include validation of RNA sequencing data with quantitative polymerase chain reaction (qPCR), which would provide confirmation of the gene expression data as to whether the regulatory trends observed in RNA

sequencing were legitimate trends or produced by artifacts in sequencing or library preparation. In addition, this work sets the foundation for future studies evaluating the cytotoxicity of various nanomaterials in both gram negative and gram positive bacteria, providing standard operating procedures and handling protocols for the various assays and techniques in the evaluation of microbial cytotoxicity.

Table 4. Overview of current studies on SWCNT cytotoxicity

Functionalization	Diameter; Length	Concentration	Exposure time	Cell line	Cytotoxicity	Notes	Reference
n-propylamine, phenylhydrazine, hydroxy, phenyldicarboxy, phenyl, sulfonic acid, *n*-butyl, diphenylcyclopropane, hydrazine	0.35 nm - 1.1 nm; > 1 µm	0.5 mg of each CNT type coated onto 0.5 µm pore PTFE membrane	0.5 h	*E. coli*	62.2 ± 5.3 to 92.4 ± 2.7 % cell viability loss	Cytotoxicity was not directcly correlated to any specific physiochemcial property, but rather indirectly correlated to aggregrate size	Pasquini et al. 2012
None	0.83 nm; 1 µm	5-80 µg/mL	2 h	*E. coli*, *Pseudomonas aeruginosa*, *Staphylococcus aureus*, *Bacillus subtilis*	Death rate ≤ 53.9 ± 2.8 % in saline	Higher cytotoxicity for individually dispersed SWCNTs than for aggregated SWCNTs	Liu et al. 2009
Unknown	0.7 nm -2.5 nm: 0.5 µm -10 µm	0.3 mg/mL -1.5 mg/mL	≤ 2 h	*Salmonella enteria*, *E. coli*	Growth curves show lower final OD_{600} with exposure ≥ 0.3 mg/mL	Sodium cholate was the surfactant with lowest cytotoxicity; Growth plateau after SWCNT treatment	Dong et al. 2011

Table 4 continued. Overview of current studies on SWCNT cytotoxicity

Functionalization	Diameter; Length	Concentration	Exposure time	Cell line	Cytotoxicity	Notes	Reference
phenyl-SO_3H, phenyl-SO_3Na, phenyl-$(COOH)_2$, none	1 nm; 400 nm	3 μg/mL to 30 mg/mL	48 h	Human dermal fibroblasts	Cell death ≤ 50% functionalized SWCNTs	As degree of functionalizaed increased, cytotoxicity decreased	Sayes et al. 2006
OH	1 nm -1.5 nm; 1 μm, 1-5 μm, 5 μm	50 μg/mL to 200 μg/mL	≤ 5 h	*Salmonella typhimurium*	≤ 4.38 log reduction in CFU/mL	CNTs had 4.07 % content of impurities (Na, Al, Si, A, Fe); Longer SWCNTs had higher cytotoxicity	Yang et al. 2010
None	1.4 nm; 1 μm	1.41 μg/mL to 226 μg/mL	6 h	Guinea pig alveolar macrophages	> 20 % inhibition at 1.41 μg/mL	CNTs had ~ 10 % impurites (including trace amounts of Fe, Ni, Y); SWCNT found to inhibit	Jia et al. 2005
OH, COOH	1.5 nm; 10 μm	25 μg/mL to 200 μg/mL	1 h	*S. typhimurium*, *S. aureus*, *B. subtilis*	Antibacterial activity at ≥ 50 μg/mL in water and saline	Cytotoxicity dependant on CNT concentration and buffer used	Arias and Yang 2009

Table 4 continued. Overview of current studies on SWCNT cytotoxicity

Functionalization	Diameter; Length	Concentration	Exposure time	Cell line	Cytotoxicity	Notes	Reference
None	0.9 nm; 2 μm	0.6 mg CNT coated onto 5 μm pore PVDF membrane; 5 μg/mL in saline	2 h	*E. coli*	1001 differentialy expressioned genes (≥ 2-fold change); 91 % of upregulated genes stress-related	Demonstrates diameter dependance of cytotoxicty; SWCNT cause higher expression of stress related gene products	Kang et al. 2008
COOH	1 nm-5 nm; 0.1 μm – 1 μm	0.5 mg/mL	1 h	Human promyelcytic leukemia cells, HL60, Jurkat T cells	Not determined	No significant cytotoxicity in COOH functionalized SWCNTs	Kam et al. 2004
None	0.9 nm; 1 μm- 3 μm	1 μg/mL- 50 μg/mL	≤ 2 h	*E. coli*	Loss of cell viability ≤ 87.6 ± 4.7 %	Cell membrane damage caused by SWCNTs possible mechanism for observed cytotoxicity	Kang et al. 2007

5 REFERENCES

Agilent Technologies. 2005. "Agilent 2100 bioanalyzer 2100 expert user's guide. Manuals and product inserts." 2005. http://www.chem.agilent.com/library/usermanuals/Public/G2946-90004_Vespucci_UG_eBook_%28NoSecPack%29.pdf.

Akmrud JJ, Kern AD, Wang SC, Czerwinski RM, Johnson WH Jr, Murzin AG, Hackert ML, Whitman CP. 2002. The crystal structure of YdcE, a 4-oxalocrotonate tautomerase homologue from *Escherichia coli*, confirms the structural basis for oligomer diversity. Biochemistry. **41**(40):12010-12024.

Arias LR, Yang L. 2009. Inactivation of Bacterial Pathogens by Carbon Nanotubes in Suspensions. Langmuir. **25**(5):3003-3012.

Beloin C, Roux A, Ghigo J-M. 2008. *Escherichia coli* biofilms. Curr Top Microbiol Immunol. **322**:249-289.

Benjamini Y, Hochberg Y. 1995. Controlling the false discovery rate: a practical and powerful approach to multiple testing. J R Stat Soc Series B Stat Methodol. **57:**289-300.

Bianco A, Kostarelos K, Prato M. 2005. Applications of carbon nanotubes in drug delivery. Curr Opin Chem Biol. **9**(6):674-679.

Bosi S, Da Ros T, Spalluto G, Balzarini J, Prato M. 2003. Synthesis and anti-HIV properties of new water-soluble bis-functionalized[60]fullerene derivatives. Bioorg Med Chem Lett. **13**(24):4437-4440.

Cai D, Mataraza JM, Qin ZH, Huang Z, Huang J, Chiles TC, Carnahan D, Kempa K, Ren Z. 2005. Highly efficient molecular delivery into mammalian cells using carbon nanotube spearing. Nat Methods. **2**(6):449-454.

Chen H, Wang B, Gao D, Guan M, Zheng L, Ouyang H, Chai Z, Zhao Y, Feng W. 2013. Broad-Spectrum Antibacterial Activity of Carbon Nanotubes to Human Gut Bacteria. Small. **9**(16):2735-2746.

Chen L, Xie H, Yu W. 2011. Functionalization methods of carbon nanotubes and its applications, p 213-232. *In* Marulanda, J M (ed), Carbon Nanotubes Applications on Electron Devices. InTech, New York.

Chen RJ, Bangsaruntip S, Drouvalakis KA, Kam NWS, Shim M, Li Y, Kim W, Utz PJ, Dai H. 2003. Noncovalent functionalization of carbon nanotubes for highly specific electronic biosensors. Proc Natl Acad Sci USA. **100**(9):4984-4989.

Dai H. 2002. Carbon nanotubes: synthesis, integration, and properties. Accounts Chem Res. **35**:1035–1044.

De Souza AA, Takita MA, Coletta-Filho HD, Caldana C, Yanai GM, Muto NH, De Oliveira RC, Nunes LR, Machado MA. 2004. Gene expression profile of the plant pathogen Xylella fastidiosa during biofilm formation in vitro. FEMS Microbiol Lett. **237**(2):341-353.

De Volder MF, Tawfick SH, Baughman R H, Hart AJ. 2013. Carbon nanotubes: present and future commercial applications. Science. **339**(6119):535-539.

Dong L, Henderson A, Field C. 2011. Antimicrobial activity of single-walled carbon nanotubes suspended in different surfactants. J Nanotechnology. **2012**:doi:10.1155/2012/928924.

Gaudy Jr. AF, Abu-Niaaj F, Gaudy ET. 1963. Statistical Study of the Spot-Plate Technique for Viable-Cell Counts. Appl Microbiol. **11**(4):305–309.

Giannoukos G, Ciulla DM, Huang K, Haas BJ, Izard J, Levin JZ, Livny J, Earl AM, Gevers D, Ward DV, Nusbaum C, Birren BW, Gnirke A. 2012. Efficient and robust RNA-seq process for cultured bacteria and complex community transcriptomes. Genome Biol. **13**(3):R23.

Grujicic M, Gao G, Rao AM, Tritt TM, Nayak S. 2003. UV-lightenhanced oxidation of carbon nanotubes. Appl Surf Sci. **214**:289– 303.

Herzberg M, Kaye IK, Peti W, Wood TK. 2006. YdgG (TqsA) controls biofilm formation in *Escherichia coli* K-12 through autoinducer 2 transport. J Bacteriol. **188**(2):587-598.

Huang TS, Tzeng Y, Liu YK, Chen YC, Walker KR, Guntupalli R, Liu C. 2004. Immobilization of antibodies and bacterial binding on nanodiamond and carbon nanotubes for biosensor applications. Diam Relat Mater. **13**(4):1098-1102.

Imuta N, Nishi J, Tokuda K, Fujiyama R, Manago K, Iwashita M, Sarantuya J, Kawano, Y. 2008. The *Escherichia coli* efflux pump TolC promotes aggregation of enteroaggregative *E. coli* 042. Infection and immunity. **76**(3):1247-1256.

Jensen AW, Wilson SR, Schuster DI. 1996. Biological applications of fullerenes. Bioorg Med Chem. **4**(6):767-779.

Jia G, Wang H, Yan L, Wang X, Pei R, Yan T, Zhao Y, Guo X. 2005. Cytotoxicity of carbon nanomaterials: single-wall nanotube, multi-wall nanotube, and fullerene. Environ Sci Technol. **39**:1378–1383.

Kam N, Jessop T, Wender P, Dai H. 2004. Nanotube Molecular Transporters: Internalization of Carbon Nanotube−Protein Conjugates into Mammalian Cells. J Am Chem Soc. **126**:6850–6851.

Kam NW, O'Connell M, Wisdom JA, Dai H. 2005. Carbon nanotubes as multifunctional biological transporters and near-infrared agents for selective cancer cell

destruction**.** Proc Natl Acad Sci USA. 102(33):1160-11605.

Kanehisa M, Goto S. 2000. KEGG: Kyoto Encyclopedia of Genes and Genomes. Nucleic Acids Res. **28**(1):27–30.doi:10.1093/nar/28.1.27.

Kang S, Herzberg M, Rodrigues DF, Elimelech M. 2008. Antibacterial effects of carbon nanotubes: size does matter!. Langmuir. **24**(13):6409-6413.

Kang S, Pinault M, Pfefferle LD, Elimelech M. 2007. Single-walled carbon nanotubes exhibit strong antimicrobial activity. Langmuir **23**:8670–8673.

Kim J, Song K, Lee J, Choi Y, Bang I, Kang C, Yu I. 2012. Toxicogenomic comparison of multi-wall carbon nanotubes (MWCNTs) and asbestos. Arch Toxicol. **86**:553–562.

Kirby JE, Trempy JE, Gottlesman S. 1994. Excision of a P4-like cryptic prophage leads to Alp protease expression in *Escherichia coli*. J Bacteriol. **176**(7):2066-2081.

Köhler AR, Som C, Helland A, Gottschalk F. 2008. Studying the potential release of carbon nanotubes throughout the application life cycle. J Clean Prod. ***16***(8):927-937.

Kolosnjaj-Tabi J, Szwarc H, Moussa F. 2012. In vivo toxicity studies of pristine carbon nanotubes: a review. Del Nanoparticles. **2000**:37-58.

Lewinski N, Colvin V, Drezek R. 2008. Cytotoxicity of nanoparticles. Small. **4**(1):26-49.

Liu S, Wei L, Hao L, Fang N, Chang MW, Xu R, Yang Y, Chen Y. 2009. Sharper and faster "nano darts" kill more bacteria: a study of antibacterial activity of individually dispersed pristine single-walled carbon nanotube. ACS Nano **3**:3891–3902.

Liu T, Tang H, Zhao J, Li D, Li R, Sun X. 2007. A study on the bactericidal properties of Cu-coated carbon nanotubes. Front Mater Sci China. **1**(2):147-150.

Marchler-Bauer A, Derbyshire MK, Gonzales NR, Lu S, Chitsaz F, Geer LY, Geer RC, He J, Gwadz M, Hurwitz DI, Lanczycki CJ, Lu F, Marchler GH, Song JS, Thanki N, Wang Z, Yamashita RA, Zhang D, Zheng C, Bryant SH. 2015. CDD: NCBI's conserved domain database. Nucleic Acids Res. **43**:doi:10.1093/nar/gku1221.D222-6.

Oberdörster G, Oberdörster E, Oberdörster J. 2005. Nanotoxicology: an emerging discipline evolving from studies of ultrafine particles. Environ Health Perspect. **113**(7):823-839.

Park SY, Cromie MJ, Lee EJ, Groisman EA. 2010. A bacterial mRNA leader that employs different mechanisms to sense disparate intracellular signals. Cell. **142**(5):737-748.

Pasquini LM, Hashmi SM, Sommer TJ, Elimelech M, Zimmerman JB. 2012. Impact of surface functionalization on bacterial cytotoxicity of single-walled carbon nanotubes. Environ Sci Technol. **46**(11):6297-6305.

Petersen EJ, Zhang L, Mattison NT, O'Carroll DM, Whelton AJ, Uddin N, Nguyen T, Huang Q, Henry TB, Holbrook RD, Chen KL. 2011. Potential release pathways, environmental fate, and ecological risks of carbon nanotubes. Environ Sci Technol. **45**:9837–9856.

Puretzky AA, Geohegan DB, Fan X, Pennycook SJ. 2000. Dynamics of single-wall carbon nanotube synthesis by laser vaporization. Appl Phys A. **70**:153-160.

Reinhart DR, Berge ND, Santra S, Bolyard SC. 2010. Emerging contaminants: Nanomaterial fate in landfills. Waste Manage. **30**(11):2020-2021.

Riley M, Abe T, Arnaud MB, Berlyn MK, Blattner FR, Chaudhuri RR, Glasner JD, Horiuchi T, Keseler IM, Kosuge T, Mori H, Perna NT, Plunkett G 3rd, Rudd KE, Serres MH, Thomas GH, Thomson NR, Wishart D, Wanner BL. 2006. Escherichia coli K-12: a cooperatively developed annotation snapshot—2005. Nucleic acids res. **34**(1):1-9.

Sayes CM, Liang F, Hudson JL, Mendez J, Guo W, Beach JM, Moore VC, Doyle CD, West JL, Billups WE, Ausman KD, Colvin VL. 2006. Functionalization density dependence of single-walled carbon nanotubes cytotoxicity in vitro. Toxicol Lett. **161**:135–142.

Timur S, Anik U, Odaci D, Gorton L. 2007. Development of a microbial biosensor based on carbon nanotube (CNT) modified electrodes. Electrochem Commun. **9**(7):1810-1815.

Trojanowicz M. 2006. Analytical applications of carbon nanotubes: a review. Trac-Trend Anal Chem. **25**(5):480-489.

United States Environmental Protection Agency. 2010. Emerging contaminants-nanomaterials. United States Environmental Protection Agency.

United States Environmental Protection Agency. Significant new use rules on certain chemical substances. 2 Feb 2015. Pp 5457 -5471. https://federalregister.gov/a/2015-01721.

United States Environmental Protection Agency. 2008. TSCA inventory status of nanoscale substances- general approach. United States Environmental Protection Agency.

Yang C, Mamouni J, Tang Y, Yang L. 2010. Antimicrobial activity of single-walled carbon nanotubes: length effect. Langmuir. **26**(20):16013-16019.

Wang J, Musameh M, Lin Y. 2003. Solubilization of carbon nanotubes by Nafion toward the preparation of amperometric biosensors. J Am Chem Soc. **125**(9):2408-2409.

Webb JS, Thompson LS, James S, Charlton T, Tolker-Nielsen T, Koch B, Givskov M, Kjelleberg S. 2003. Cell Death in Pseudomonas aeruginosa Biofilm Development. J Bacteriol. **185**(15):4585-4592.

Whitman CP. 2002. The 4-oxalocrotonate tautomerase family of enzymes: how nature makes new enzymes using a beta-alpha-beta structural motif. Arch Biochem Biophys. **402**(1):1-13.

Wiegand I, Hilpert K, Hancock REW. 2008. Agar and broth dilution methods to determine the minimal inhibitory concentration (MIC) of antimicrobial substances. Nat Protoc. **3**:163–175.

Yun Y, Dong Z, Shanov VN, Schulz MJ. 2007. Electrochemical impedance measurement of prostate cancer cells using carbon nanotube array electrodes in a microfluidic channel. Nanotechnology. **18**:doi:10.1088/0957-4484/18/46/465505.